MitoFit Preprint Arch (2019) doi:10.26124/mitofit:190001.v4
Posted online 2019-05-20 Open Access freely available online

Mitochondrial respiratory states and rates

Gnaiger E, Aasander Frostner E, Abdul Karim N, Abumrad NA, Acuna-Castroviejo D, Adiele RC, Ahn B, Ali SS, Almeida A, Alton L, Alves MG, Amati F, Amoedo ND, Andreadou I, Aragó M, Aral C, Arandarčikaitė O, Armand AS, Arnould T, Avram VF, Bailey DM, Bajpeyi S, Bajzikova M, Bakker BM, Barlow J, Bastos Sant'Anna Silva AC, Batterson P, Battino M, Bazil J, Beard DA, Bednarczyk P, Bello F, Ben-Shachar D, Bento G, Bergdahl A, Berge RK, Bergmeister L, Bernardi P, Berridge MV, Bettinazzi S, Bishop D, Blier PU, Blindheim DF, Boardman NT, Boetker HE, Borchard S, Boros M, Børsheim E, Borutaite V, Botella J, Bouillaud F, Bouitbir J, Boushel RC, Bovard J, Breton S, Brown DA, Brown GC, Brown RA, Brozinick JT, Buettner GR, Burtscher J, Calabria E, Calbet JA, Calzia E, Cannon DT, Cano Sanchez M, Canto AC, Cardoso LHD, Carvalho E, Casado Pinna M, Cassar S, Cassina AM, Castelo MP, Castro L, Cavalcanti-de-Albuquerque JP, Cervinkova Z, Chabi B, Chakrabarti L, Chakrabarti S, Chaurasia B, Chen Q, Chicco AJ, Chinopoulos C, Chowdhury SK, Cizmarova B, Clementi E, Coen PM, Cohen BH, Coker RH, Collin A, Crisóstomo L, Dahdah N, Dalgaard LT, Dambrova M, Danhelovska T, Darveau CA, Das AM, Dash RK, Davidova E, Davis MS, De Goede P, De Palma C, Dembinska-Kiec A, Detraux D, Devaux Y, Di Marcello M, Dias TR, Diederich M, Distefano G, Doermann N, Doerrier C, Dong L, Donnelly C, Drahota Z, Duarte FV, Dubouchaud H, Duchen MR, Dumas JF, Durham WJ, Dymkowska D, Dyrstad SE, Dyson A, Dzialowski EM, Eaton S, Ehinger J, Elmer E, Endlicher R, Engin AB, Escames G, Ezrova Z, Falk MJ, Fell DA, Ferdinandy P, Ferko M, Ferreira JCB, Ferreira R, Ferri A, Fessel JP, Filipovska A, Fisar Z, Fischer C, Fischer M, Fisher G, Fisher JJ, Ford E, Fornaro M, Galina A, Galkin A, Gallee L, Galli GL, Gama Pérez P, Gan Z, Ganetzky R, Garcia-Rivas G, Garcia-Roves PM, Garcia-Souza LF, Garipi E, Garlid KD, Garrabou G, Garten A, Gastaldelli A, Gayen J, Genders AJ, Genova ML, Giovarelli M, Goncalo Teixeira da Silva R, Goncalves DF, Gonzalez-Armenta JL, Gonzalez-Freire M, Gonzalo H, Goodpaster BH, Gorr TA, Gourlay CW, Granata C, Grefte S, Guarch ME, Gueguen N, Gumeni S, Haas CB, Haavik J, Haendeler J, Haider M, Hamann A, Han J, Han WH, Hancock CR, Hand SC, Handl J, Hargreaves IP, Harper ME, Harrison DK, Hassan H, Hausenloy DJ, Heales SJR, Hecker M, Heiestad C, Hellgren KT, Hepple RT, Hernansanz-Agustin P, Hewakapuge S, Hickey AJ, Ho DH, Hoehn KL, Hoel F, Holland OJ, Holloway GP, Hoppel CL, Hoppel F, Houstek J, Huete-Ortega M, Hyrossova P, Iglesias-Gonzalez J, Irving BA, Isola R, Iyer S, Jackson CB, Jadiya P, Jana PF, Jang DH, Jang YC, Janowska J, Jansen K, Jansen-Dürr P, Jansone B, Jarmuszkiewicz W, Jaskiewicz A, Jedlicka J, Jespersen NR, Jha RK, Jones JG, Jurczak MJ, Jurk D, Jusic A, Kaambre T, Kaczor JJ, Kainulainen H, Kampa RP, Kandel SM, Kane DA, Kapferer W, Kappler L, Karabatsiakis A, Karavaeva I, Karkucinska-Wieckowska A, Kaur S, Keijer J, Keller MA, Keppner G, Khamoui AV, Kidere D, Kilbaugh T, Kim HK, Kim JKS, Klepinin A, Klepinina L, Klingenspor M, Klocker H, Komlodi T, Koopman WJH, Kopitar-Jerala N, Kowaltowski AJ, Kozlov AV, Krajcova A, Krako Jakovljevic N, Kristal BS, Krycer JR, Kuang J, Kucera O, Kuka J, Kwak HB, Kwast K, Laasmaa M, Labieniec-Watala M, Lagarrigue S, Lai N, Land JM, Lane N, Laner V, Lanza IR, Laranjinha J, Larsen TS, Lavery GG, Lazou A, Lee HK, Leeuwenburgh C, Lehti M, Lemieux H, Lenaz G, Lerfall J, Li PA, Li Puma L, Liepins E, Liu J, López LC, Lucchinetti E, Ma T, Macedo MP, Maciej S, MacMillan-Crow LA, Majtnerova P, Makarova E, Makrecka-Kuka M, Malik AN, Markova M, Martin DS, Martins AD, Martins JD, Maseko TE, Maull F, Mazat JP, McKenna HT, McKenzie M, Menze MA, Merz T, Meszaros AT, Methner A, Michalak S, Moellering DR, Moisoi N, Molina AJA, Montaigne D, Moore AL, Moreau K, Moreno-Sánchez R, Moreira BP, Mracek T, Muccini AM, Munro D, Muntane J, Muntean DM, Murray AJ, Musiol E, Nabben M, Nair KS, Nehlin JO, Nemec M, Neufer PD, Neuzil J, Neviere R, Newsom SA, Nozickova K, O'Brien KA, O'Gorman D, Olgar Y, Oliveira B, Oliveira MF, Oliveira MT, Oliveira PF, Oliveira PJ, Orynbayeva Z, Osiewacz HD, Pak YK, Pallotta ML, Palmeira CM, Parajuli N, Passos JF, Passrugger M, Patel HH, Pavlova N, Pecina P, Pedersen TM, Pereira da Silva Grilo da Silva F, Pereira SP, Perez Valencia JA, Perks KL, Pesta D, Petit PX, Pettersen IKN, Pichaud N, Pichler I, Piel S, Pietka TA, Pino

MF, Pirkmajer S, Plangger M, Porter C, Porter RK, Prigione A, Procaccio V, Prochownik EV, Prola A, Pulinilkunnil T, Puskarich MA, Puurand M, Radenkovic F, Ramzan R, Rattan SIS, Reboredo P, Renner-Sattler K, Rial E, Robinson MM, Roden M, Rodriguez E, Rodriguez-Enriquez S, Rohlena J, Rolo AP, Ropelle ER, Røsland GV, Rossignol R, Rossiter HB, Rubelj I, Rybacka-Mossakowska J, Saada A, Safaei Z, Saharnaz S, Salin K, Salvadego D, Sandi C, Saner N, Sanz A, Sazanov LA, Scatena R, Schartner M, Scheibye-Knudsen M, Schilling JM, Schlattner U, Schönfeld P, Schots PC, Schulz R, Schwarzer C, Scott GR, Selman C, Shabalina IG, Sharma P, Sharma V, Shevchuk I, Shirazi R, Shiroma JG, Siewiera K, Silber AM, Silva AM, Sims CA, Singer D, Singh BK, Skolik R, Smenes BT, Smith J, Soares FAA, Sobotka O, Sokolova I, Sommer N, Sonkar VK, Sowton AP, Sparagna GC, Sparks LM, Spinazzi M, Stankova P, Starr J, Stary C, Stelfa G, Stepto NK, Stiban J, Stier A, Stocker R, Storder J, Sumbalova Z, Suomalainen A, Suravajhala P, Svalbe B, Swerdlow RH, Swiniuch D, Szabo I, Szewczyk A, Szibor M, Tanaka M, Tandler B, Tarnopolsky MA, Tausan D, Tavernarakis N, Tepp K, Thakkar H, Thapa M, Thyfault JP, Tomar D, Ton R, Torp MK, Towheed A, Tretter L, Trewin AJ, Trifunovic A, Trivigno C, Tronstad KJ, Trougakos IP, Truu L, Tuncay E, Turan B, Tyrrell DJ, Urban T, Valentine JM, Van Bergen NJ, Van Hove J, Varricchio F, Vella J, Vendelin M, Vercesi AE, Victor VM, Vieira Ligo Teixeira C, Vidimce J, Viel C, Vieyra A, Vilks K, Villena JA, Vincent V, Vinogradov AD, Viscomi C, Vitorino RMP, Vogt S, Volani C, Volska K, Votion DM, Vujacic-Mirski K, Wagner BA, Ward ML, Warnsmann V, Wasserman DH, Watala C, Wei YH, Weissig V, Whitfield J, Wickert A, Wieckowski MR, Wiesner RJ, Williams CM, Winwood-Smith H, Wohlgemuth SE, Wohlwend M, Wolff JN, Wrutniak-Cabello C, Wüst RCI, Yokota T, Zablocki K, Zanon A, Zanou N, Zaugg K, Zaugg M, Zdrazilova L, Zhang Y, Zhang YZ, Zíková A, Zischka H, Zorzano A, Zvejniece L

Corresponding author: Gnaiger E
Chair COST Action CA15203 MitoEAGLE – http://www.mitoeagle.org
Department of Visceral, Transplant and Thoracic Surgery, D. Swarovski Research Laboratory, Medical University of Innsbruck, Innrain 66/4, A-6020 Innsbruck, Austria
Email: mitoeagle@i-med.ac.at; *Tel: +43 512 566796, Fax: +43 512 566796 20*

542 coauthors

MitoEAGLE Task Group, COST Action CA15203 MitoEAGLE

http://www.mitofit.org/index.php/Gnaiger_2019_MitoFit_Preprint_Arch

EUROPEAN COOPERATION IN SCIENCE & TECHNOLOGY

Funded by the Horizon 2020 Framework Programme of the European Union

Editor MitoFit Preprint Archives: Gnaiger E

Table of contents

Abstract As the knowledge base and importance of mitochondrial physiology to human health expands, the necessity for harmonizing the terminology concerning mitochondrial respiratory states and rates has become increasingly apparent. The chemiosmotic theory establishes the mechanism of energy transformation and coupling in oxidative phosphorylation. The unifying concept of the protonmotive force provides the framework for developing a consistent theoretical foundation of mitochondrial physiology and bioenergetics. We follow guidelines of the International Union of Pure and Applied Chemistry (IUPAC) on terminology in physical chemistry, extended by considerations of open systems and thermodynamics of irreversible processes. The concept-driven constructive terminology incorporates the meaning of each quantity and aligns concepts and symbols with the nomenclature of classical bioenergetics. We endeavour to provide a balanced view of mitochondrial respiratory control and a critical discussion on reporting data of mitochondrial respiration in terms of metabolic flows and fluxes. Uniform standards for evaluation of respiratory states and rates will ultimately contribute to reproducibility between laboratories and thus support the development of databases of mitochondrial respiratory function in species, tissues, and cells. Clarity of concept and consistency of nomenclature facilitate effective transdisciplinary communication, education, and ultimately further discovery.

Keywords: Mitochondrial respiratory control, coupling control, mitochondrial preparations, protonmotive force, uncoupling, oxidative phosphorylation: OXPHOS, efficiency, electron transfer: ET, electron transfer system: ETS, proton leak, ion leak and slip compensatory state: LEAK, residual oxygen consumption: ROX, State 2, State 3, State 4, normalization, flow, flux, oxygen: O_2

Executive summary

In view of the broad implications for health care, mitochondrial researchers face an increasing responsibility to disseminate their fundamental knowledge and novel discoveries to a wide range of stakeholders and scientists beyond the group of specialists. This requires implementation of a commonly accepted terminology within the discipline and standardization in the translational context. Authors, reviewers, journal editors, and lecturers are challenged to collaborate with the aim to harmonize the nomenclature in the growing field of mitochondrial physiology and bioenergetics, from evolutionary biology and comparative physiology to mitochondrial medicine. In the present communication we focus on the following concepts in mitochondrial physiology:

1. Aerobic respiration is the O_2 flux in catabolic reactions coupled to phosphorylation of ADP to ATP, and O_2 flux in a variety of O_2 consuming reactions apart from oxidative phosphorylation (OXPHOS). Coupling in OXPHOS is mediated by the translocation of protons across the mitochondrial inner membrane (mtIM) through proton pumps generating or utilizing the protonmotive force that is maintained between the mitochondrial matrix and intermembrane compartment or outer mitochondrial space. Compartmental coupling depends on ion translocation across a semipermeable membrane, which is defined as vectorial metabolism and distinguishes OXPHOS from cytosolic fermentation as counterparts of cellular core energy metabolism (**Figure 1**). Cell respiration is thus distinguished from fermentation: (*1*) Electron acceptors are supplied by external respiration for the maintenance of redox balance, whereas fermentation is characterized by an internal electron acceptor produced in intermediary metabolism. In aerobic cell respiration, redox balance is maintained by O_2 as the electron acceptor. (*2*) Compartmental coupling in vectorial OXPHOS contrasts to exclusively scalar substrate-level phosphorylation in fermentation.
2. When measuring mitochondrial metabolism, the contribution of fermentation and other cytosolic interactions must be excluded from analysis by disrupting the barrier function of the plasma membrane. Selective removal or permeabilization of the plasma membrane yields mitochondrial preparations—including isolated mitochondria, tissue and cellular preparations—with structural and functional integrity. Subsequently, extra-mitochondrial concentrations of fuel substrates, ADP, ATP, inorganic phosphate, and cations including H^+ can be controlled to determine mitochondrial function under a set of conditions defined as coupling control states. We strive to incorporate an easily recognized and understood concept-driven terminology of bioenergetics with explicit terms and symbols that define the nature of respiratory states.

3. Mitochondrial coupling states are defined according to the control of respiratory oxygen flux by the protonmotive force, pmf, in an interaction of the electron transfer system generating the pmf and the phosphorylation system utilizing the pmf. Capacities of OXPHOS and electron transfer are measured at kinetically-saturating concentrations of fuel substrates, ADP and inorganic phosphate, and O_2, or at optimal uncoupler concentrations, respectively, in the absence of Complex IV inhibitors such as NO, CO, or H_2S. Respiratory capacity is a measure of the upper boundary of the rate of respiration; it depends on the substrate type undergoing oxidation in a mitochondrial pathway, and provides reference values for the diagnosis of health and disease. Evaluation of the impact of **E**volutionary background, **A**ge, **G**ender and sex, **L**ifestyle and **E**nvironment represents a major challenge for mitochondrial respiratory physiology and pathology.

Figure 1. Internal and external respiration

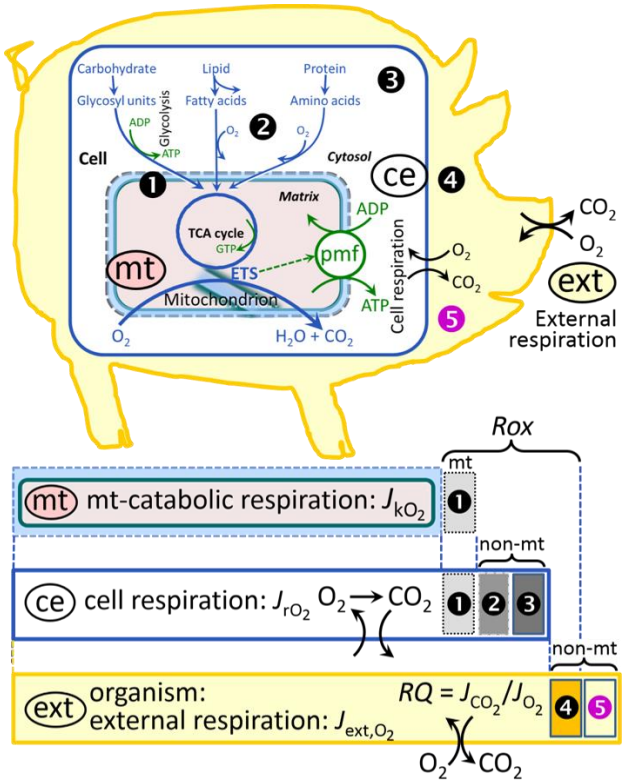

(mt) **Mitochondrial catabolic respiration**, J_{kO_2}, is the O_2 consumption in the oxidation of fuel substrates (electron donors) and reduction of O_2 catalysed by the electron transfer system, ETS, excluding (❶) mitochondrial residual oxygen consumption, mt-*Rox*.

(ce) **Cell respiration** or internal cellular O_2 consumption, J_{rO_2}, takes into account all chemical reactions, r, that consume O_2 in the cells. Catabolic cell respiration is the O_2 consumption associated with catabolic pathways in the cell, including (mt) mitochondrial catabolism; (❶) mt-*Rox*; (❷) non-mt O_2 consumption by catabolic reactions, particularly peroxisomal oxidases and microsomal cytochrome P450 systems; and (❸) non-mt *Rox* by reactions unrelated to catabolism.

(ext) **External respiration** balances internal respiration at steady-state, including (❹) extracellular *Rox* and (❺) aerobic respiration by the microbiome. O_2 is transported from the environment across the respiratory cascade, *i.e.*, circulation between tissues and diffusion across cell membranes, to the intracellular compartment. The respiratory quotient, *RQ*, is the molar CO_2/O_2 exchange ratio; when combined with the respiratory nitrogen quotient, N/O_2 (mol N given off per mol O_2 consumed), the *RQ* reflects the proportion of carbohydrate, lipid and protein utilized in cell respiration during aerobically balanced steady-states. Bicarbonate and CO_2 are transported in reverse to the extracellular mileu and the organismic environment. Hemoglobin provides the molecular paradigm for the combination of O_2 and CO_2 exchange, as do lungs and gills on the morphological level. Consult **Table 8** for a list of terms and symbols.

4. Incomplete tightness of coupling, *i.e.*, some degree of uncoupling relative to the mitochondrial pathway-dependent coupling stoichiometry, is a characteristic of energy-transformations across membranes. Uncoupling is caused by a variety of physiological, pathological, toxicological, pharmacological and environmental conditions that exert an influence not only on the proton leak and cation cycling, but also on proton slip within the proton pumps and the structural integrity of the mitochondria. A more loosely coupled state is induced by stimulation of mitochondrial superoxide formation and the bypass of proton pumps. In addition, the use of protonophores represents an experimental uncoupling intervention to assess the transition from a well-coupled to a noncoupled state of mitochondrial respiration.
5. Respiratory oxygen consumption rates have to be carefully normalized to enable meta-analytic studies beyond the question of a particular experiment. Therefore, all raw data on rates and variables for normalization should be published in an open access data repository.

Normalization of rates for: (*1*) the number of objects (cells, organisms); (*2*) the volume or mass of the experimental sample; and (*3*) the concentration of mitochondrial markers in the instrumental chamber are sample-specific normalizations, which are distinguished from system-specific normalization for the volume of the instrumental chamber (the measuring system).

6. The consistent use of terms and symbols facilitates transdisciplinary communication and will support the further development of a collaborative database on bioenergetics and mitochondrial physiology.

Box 1: In brief – Mitochondria and Bioblasts

> '*For the physiologist, mitochondria afforded the first opportunity for an experimental approach to structure-function relationships, in particular those involved in active transport, vectorial metabolism, and metabolic control mechanisms on a subcellular level*' (Ernster and Schatz 1981).

Mitochondria are oxygen-consuming electrochemical generators that evolved from the endosymbiotic alphaproteobacteria which became integrated into a host cell related to Asgard Archaea (Margulis 1970; Lane 2005; Roger *et al.* 2017). They were described by Richard Altmann (1894) as 'bioblasts', which include not only the mitochondria as presently defined, but also symbiotic and free-living bacteria. The word 'mitochondria' (Greek mitos: thread; chondros: granule) was introduced by Carl Benda (1898). Mitochondrion is singular and mitochondria is plural. Abbreviation: mt, as generally used in mtDNA.

Contrary to current textbook dogma, which describes mitochondria as individual organelles, mitochondria form dynamic networks within eukaryotic cells. Mitochondrial movement is supported by microtubules. Mitochondrial size and number can change in response to energy requirements of the cell via processes known as fusion and fission; these interactions allow mitochondria to communicate within a network (Chan 2006). Mitochondria can even traverse cell boundaries in a process known as horizontal mitochondrial transfer (Torralba *et al.* 2016). Another defining morphological characteristic of mitochondria is the double membrane. The mitochondrial inner membrane (mtIM) forms dynamic tubular to disk-shaped cristae that separate the mitochondrial matrix, *i.e.*, the negatively charged internal mitochondrial compartment, from the intermembrane space; the latter being enclosed by the mitochondrial outer membrane (mtOM) and positively charged with respect to the matrix.

Intracellular stress factors may cause shrinking or swelling of the mitochondrial matrix that can ultimately result in permeability transition (mtPT; Lemasters *et al.* 1998). The mtIM contains the non-bilayer phospholipid cardiolipin, which is also involved in the mtOM (Gebert *et al.* 2009) but is not present in any other eukaryotic cellular membrane. Cardiolipin has many regulatory functions (Oemer *et al.* 2018); it promotes and stabilizes the formation of supercomplexes (SC $I_nIII_nIV_n$) based on dynamic interactions between specific respiratory complexes (McKenzie *et al.* 2006; Greggio *et al.* 2017; Lenaz *et al.* 2017), and it supports proton transfer on the mtIM from the electron transfer system to F-ATPase (ATP synthase; Yoshinaga *et al.* 2016). The mtIM is plastic and exerts an influence on the functional properties of incorporated proteins (Waczulikova *et al.* 2007).

Mitochondria constitute the structural and functional elementary components of cell respiration. Mitochondrial respiration is the reduction of molecular oxygen by electron transfer coupled to electrochemical proton translocation across the mtIM. In the process of OXPHOS, the catabolic reaction of oxygen consumption is electrochemically coupled to the transformation of energy in the phosphorylation of ADP to adenosine triphosphate (ATP; Mitchell 1961, 2011). Mitochondria are the powerhouses of the cell that contain the machinery of the OXPHOS-pathways, including transmembrane respiratory complexes (proton pumps with FMN, Fe-S and cytochrome *b*, *c*, aa_3 redox systems); alternative dehydrogenases and oxidases; the coenzyme ubiquinone (Q); F-ATPase or ATP synthase; the enzymes of the tricarboxylic acid cycle (TCA), fatty acid and amino acid oxidation; transporters of ions, metabolites and co-factors; iron/sulphur cluster synthesis; and mitochondrial kinases related to catabolic pathways. TCA cycle intermediates are vital precursors for macromolecule biosynthesis (Diebold *et al.* 2019). The mitochondrial proteome comprises over 1,200 proteins (Calvo *et al.* 2015; 2017), mostly encoded by nuclear DNA (nDNA), with a variety of functions, many of which are relatively well known, *e.g.*, proteins regulating mitochondrial biogenesis or apoptosis, while others are still under investigation, or need to be identified, *e.g.*, mtPT pore and alanine transporter. The

mammalian mitochondrial proteome can be used to discover and characterize the genetic basis of mitochondrial diseases (Williams *et al.* 2016; Palmfeldt and Bross 2017).

Numerous cellular processes are orchestrated by a constant crosstalk between mitochondria and other cellular components. For example, the crosstalk between mitochondria and the endoplasmic reticulum is involved in the regulation of calcium homeostasis, cell division, autophagy, differentiation, and anti-viral signaling (Murley and Nunnari 2016). Mitochondria contribute to the formation of peroxisomes, which are hybrids of mitochondrial and ER-derived precursors (Sugiura *et al.* 2017). Cellular mitochondrial homeostasis (mitostasis) is maintained through regulation at transcriptional, post-translational and epigenetic levels (Lisowski *et al.* 2018), resulting in dynamic regulation of mitochondrial turnover by biogenesis of new mitochondria and removal of damaged mitochondria by fusion, fission and mitophagy (Singh *et al.* 2018). Cell signalling modules contribute to homeostatic regulation throughout the cell cycle or even cell death by activating proteostatic modules, *e.g.*, the ubiquitin-proteasome and autophagy-lysosome/vacuole pathways; specific proteases like LON, and genome stability modules in response to varying energy demands and stress cues (Quiros *et al.* 2016). In addition, several post-translational modifications, including acetylation and nitrosylation, are capable of influencing the bioenergetic response, with clinically significant implications for health and disease (Carrico *et al.* 2018).

Mitochondria of higher eukaryotes typically maintain several copies of their own circular genome known as mitochondrial DNA (mtDNA; hundred to thousands per cell; Cummins 1998), which is maternally inherited in many species. However, biparental mitochondrial inheritance is documented in some exceptional cases in humans (Luo *et al.* 2018), is widespread in birds, fish, reptiles and invertebrate groups, and is even the norm in some bivalve taxonomic groups (Breton *et al.* 2007; White *et al.* 2008). The mitochondrial genome of the angiosperm *Amborella* contains a record of six mitochondrial genome equivalents acquired by horizontal transfer of entire genomes, two from angiosperms, three from algae and one from mosses (Rice *et al.* 2016). In unicellular organisms, *i.e.*, protists, the structural organization of mitochondrial genomes is highly variable and includes circular and linear DNA (Zikova *et al.* 2016). While some of the free-living flagellates exhibit the largest known gene coding capacity, *e.g.*, jakobid *Andalucia godoyi* mtDNA codes for 106 genes (Burger *et al.* 2013), some protist groups, *e.g.*, alveolates, possess mitochondrial genomes with only three protein-coding genes and two rRNAs (Feagin *et al.* 2012). The complete loss of mitochondrial genome is observed in the highly reduced mitochondria of *Cryptosporidium* species (Liu *et al.* 2016). Reaching the final extreme, the microbial eukaryote, oxymonad *Monocercomonoides*, has no mitochondrion whatsoever and lacks all typical nuclear-encoded mitochondrial proteins, showing that while in 99% of organisms mitochondria play a vital role, this organelle is not indispensable (Karnkowska *et al.* 2016).

In vertebrates, but not all invertebrates, mtDNA is compact (16.5 kB in humans) and encodes 13 protein subunits of the transmembrane respiratory Complexes CI, CIII, CIV and ATP synthase (F-ATPase), 22 tRNAs, and two ribosomal RNAs. Additional gene content has been suggested to include microRNAs, piRNA, smithRNAs, repeat associated RNA, long noncoding RNAs, and even additional proteins or peptides (Rackham *et al.* 2011; Duarte *et al.* 2014; Lee *et al.* 2015; Cobb *et al.* 2016). The mitochondrial genome requires nuclear-encoded mitochondrially targeted proteins, *e.g.*, TFAM, for its maintenance and expression (Rackham *et al.* 2012). The nuclear and the mitochondrial genomes encode peptides of the membrane spanning redox pumps (CI, CIII and CIV) and F-ATPase, leading to strong constraints in the coevolution of both genomes (Blier *et al.* 2001).

Given the multiple roles of mitochondria, it is perhaps not surprising that mitochondrial dysfunction is associated with a wide variety of genetic and degenerative diseases. Robust mitochondrial function is supported by physical exercise and caloric balance, and is central for sustained metabolic health throughout life. Therefore, a more consistent set of definitions for mitochondrial physiology will increase our understanding of the etiology of disease and improve the diagnostic repertoire of mitochondrial medicine with a focus on protective medicine, lifestyle and healthy aging.

---

1. Introduction

Mitochondria are the powerhouses of the cell with numerous morphological, physiological, molecular, and genetic functions (**Box 1**). Every study of mitochondrial health and disease faces

Evolution, **A**ge, **G**ender and sex, **L**ifestyle, and **E**nvironment (MitoEAGLE) as essential background conditions intrinsic to the individual person or cohort, species, tissue and to some extent even cell line. As a large and coordinated group of laboratories and researchers, the mission of the global MitoEAGLE Network is to generate the necessary scale, type, and quality of consistent data sets and conditions to address this intrinsic complexity. Harmonization of experimental protocols and implementation of a quality control and data management system are required to interrelate results gathered across a spectrum of studies and to generate a rigorously monitored database focused on mitochondrial respiratory function. In this way, researchers from a variety of disciplines can compare their findings using clearly defined and accepted international standards.

With an emphasis on quality of research, published data can be useful far beyond the specific question of a particular experiment. For example, collaborative data sets support the development of open-access databases such as those for National Institutes of Health sponsored research in genetics, proteomics, and metabolomics. Indeed, enabling meta-analysis is the most economic way of providing robust answers to biological questions (Cooper *et al.* 2009). However, the reproducibility of quantitative results and databases depend on accurate measurements under strictly-defined conditions. Likewise, meaningful interpretation and comparability of experimental outcomes requires harmonization of protocols between research groups at different institutes. In addition to quality control, a conceptual framework is also required to standardise and harmonise terminology and methodology. Vague or ambiguous jargon can lead to confusion and may convert valuable signals to wasteful noise. For this reason, measured values must be expressed in standard units for each parameter used to define mitochondrial respiratory function. A consensus on fundamental nomenclature and conceptual coherence, however, are missing in the expanding field of mitochondrial physiology. To fill this gap, the present communication provides an in-depth review on harmonization of nomenclature and definition of technical terms, which are essential to improve the awareness of the intricate meaning of current and past scientific vocabulary. This is important for documentation and integration into databases in general, and quantitative modelling in particular (Beard 2005).

In this review, we focus on coupling states and fluxes through metabolic pathways of aerobic energy transformation in mitochondrial preparations in the attempt to establish a conceptually-oriented nomenclature in bioenergetics and mitochondrial physiology in a series of communications, prepared in the frame of the EU COST Action MitoEAGLE open to global bottom-up input.

2. Coupling states and rates in mitochondrial preparations

> '*Every professional group develops its own technical jargon for talking about matters of critical concern ... People who know a word can share that idea with other members of their group, and a shared vocabulary is part of the glue that holds people together and allows them to create a shared culture*' (Miller 1991).

2.1. Cellular and mitochondrial respiration

2.1.1. Aerobic and anaerobic catabolism and ATP turnover: In respiration, electron transfer is coupled to the phosphorylation of ADP to ATP, with energy transformation mediated by the protonmotive force, pmf (**Figure 2**). Anabolic reactions are coupled to catabolism, both by ATP as the intermediary energy currency and by small organic precursor molecules as building blocks for biosynthesis (Diebold *et al.* 2019). Glycolysis involves substrate-level phosphorylation of ADP to ATP in fermentation without utilization of O_2, studied mainly in living cells and organisms. Many cellular fuel substrates are catabolized to acetyl-CoA or to glutamate, and further electron transfer reduces nicotinamide adenine dinucleotide to NADH or flavin adenine dinucleotide to $FADH_2$. Subsequent mitochondrial electron transfer to O_2 is coupled to proton translocation for the control of the protonmotive force and phosphorylation of ADP (**Figure 2B and 2C**). In contrast, extra-mitochondrial oxidation of fatty acids and amino acids proceeds partially in peroxisomes without coupling to ATP production: acyl-CoA oxidase catalyzes the oxidation of $FADH_2$ with electron transfer to O_2; amino acid oxidases oxidize flavin mononucleotide $FMNH_2$ or $FADH_2$ (**Figure 2A**).

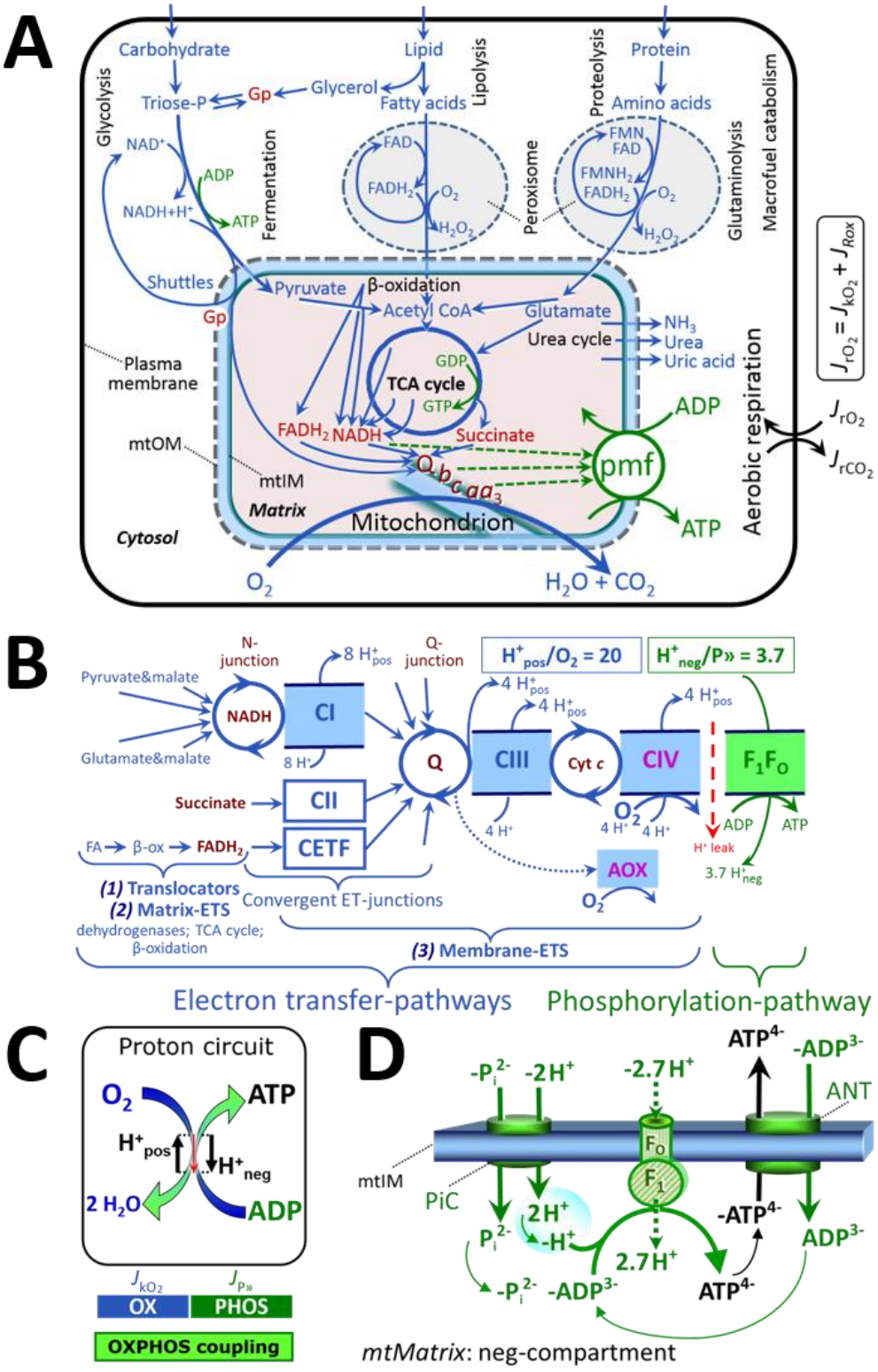

Figure 2. Cell respiration and oxidative phosphorylation (OXPHOS)
Mitochondrial respiration is the oxidation of fuel substrates (electron donors) with electron transfer to O_2 as the electron acceptor. For explanation of symbols see also **Figure 1**.
(A) Respiration of living cells: Extra-mitochondrial catabolism of macrofuels and uptake of small molecules by the cell provide the mitochondrial fuel substrates. Dashed arrows indicate the connection between the redox proton pumps (respiratory Complexes CI, CIII and CIV) and the transmembrane protonmotive force, pmf. Coenzyme Q (Q) and the cytochromes *b*, *c*, and aa_3 are redox systems of the mitochondrial inner membrane, mtIM. Glycerol-3-phosphate, Gp.

(B) Respiration in mitochondrial preparations: The mitochondrial electron transfer system (ETS) is (*1*) fuelled by diffusion and transport of substrates across the mtOM and mtIM, and in addition consists of the (*2*) matrix-ETS, and (*3*) membrane-ETS. Electron transfer converges at the N-junction, and from CI, CII and electron transferring flavoprotein complex (CETF) at the Q-junction. Unlabeled arrows converging at the Q-junction indicate additional ETS-sections with electron entry into Q through glycerophosphate dehydrogenase, dihydroorotate dehydrogenase, proline dehydrogenase, choline dehydrogenase, and sulfide-ubiquinone oxidoreductase. The dotted arrow indicates the branched pathway of oxygen consumption by alternative quinol oxidase (AOX). ET-pathways are coupled to the phosphorylation-pathway. The H^+_{pos}/O_2 ratio is the outward proton flux from the matrix space to the positively (pos) charged vesicular compartment, divided by catabolic O_2 flux in the NADH-pathway. The $H^+_{neg}/P»$ ratio is the inward proton flux from the inter-membrane space to the negatively (neg) charged matrix space, divided by the flux of phosphorylation of ADP to ATP. These stoichiometries are not fixed because of ion leaks and proton slip. Modified from Lemieux *et al*. (2017) and Rich (2013).
(C) OXPHOS coupling: The H^+ circuit couples O_2 flux through the catabolic ET-pathway, J_{kO_2}, to flux through the phosphorylation-pathway of ADP to ATP, $J_{P»}$.
(D) Phosphorylation-pathway catalyzed by the proton pump F_1F_O-ATPase (F-ATPase, ATP synthase), adenine nucleotide translocase (ANT), and inorganic phosphate carrier (PiC). The $H^+_{neg}/P»$ stoichiometry is the sum of the coupling stoichiometry in the F-ATPase reaction (-2.7 H^+_{pos} from the positive intermembrane space, 2.7 H^+_{neg} to the matrix, *i.e.*, the negative compartment) and the proton balance in the translocation of ADP^{3-}, ATP^{4-} and P_i^{2-} (negative for substrates). Modified from Gnaiger (2014).

The plasma membrane separates the intracellular compartment including the cytosol, nucleus, and organelles from the extracellular environment. Cell membranes include the plasma membrane and organellar membranes. The plasma membrane consists of a lipid bilayer with embedded proteins and attached organic molecules that collectively control the selective permeability of ions, organic molecules, and particles across the cell boundary. The intact plasma membrane prevents the passage of many water-soluble mitochondrial substrates and inorganic ions—such as succinate, adenosine diphosphate (ADP) and inorganic phosphate (P_i) that must be precisely controlled at kinetically-saturating concentrations for the analysis of mitochondrial respiratory capacities. Respiratory capacities delineate, comparable to channel capacity in information theory (Schneider 2006), the upper boundary of the rate of O_2 consumption measured in defined respiratory states. The intact plasma membrane limits the scope of investigations into mitochondrial respiratory function in living cells, despite the activity of solute carriers, *e.g.*, the sodium-dependent dicarboxylate transporter SLC13A3 and the sodium-dependent phosphate transporter SLC20A2, which transport specific metabolites across the plasma membrane of various cell types, and the availability of plasma membrane-permeable succinate (Ehinger *et al.* 2016). These limitations are overcome by the use of mitochondrial preparations.

2.1.2. Specification of biochemical dose: Substrates, uncouplers, inhibitors, and other chemical reagents are titrated to analyse cellular and mitochondrial function. Nominal concentrations of these substances are usually reported as initial amount of substance concentration [mol·L^{-1}] in the incubation medium. Kinetically-saturating conditions are evaluated by substrate kinetics to obtain the maximum reaction velocity or maximum pathway flux, in contrast to solubility-saturated conditions. When aiming at the measurement of kinetically-saturated processes—such as OXPHOS-capacities—the concentrations for substrates can be chosen according to half-saturating substrate concentrations, c_{50}, for metabolic pathways, or the Michaelis constant, K_m, for enzyme kinetics. In the case of hyperbolic kinetics, only 80% of maximum respiratory capacity is obtained at a substrate concentration of four times the c_{50}, whereas substrate concentrations of 5, 9, 19 and 49 times the c_{50} are theoretically required for reaching 83%, 90%, 95% or 98% of the maximal rate (Gnaiger 2001). Other reagents are chosen to inhibit or alter a particular process. The amount of these chemicals in an experimental incubation is selected to maximize effect, avoiding unacceptable off-target consequences that would adversely affect the data being sought. Specifying the amount of substance in an incubation as nominal concentration in the aqueous incubation medium can be ambiguous (Doskey *et al*. 2015), particularly for cations (TPP^+; fluorescent dyes such as safranin, TMRM; Chowdhury *et al.* 2015) and lipophilic substances (oligomycin, uncouplers, permeabilization agents; Doerrier *et al.* 2018), which accumulate in the

mitochondrial matrix or in biological membranes, respectively. Generally, dose/exposure can be specified per unit of biological sample, *i.e.*, (nominal moles of xenobiotic)/(number of cells) [mol·cell^{-1}] or, as appropriate, per mass of biological sample [mol·kg^{-1}]. This approach to specification of dose/exposure provides a scalable parameter that can be used to design experiments, help interpret a wide variety of experimental results, and provide absolute information that allows researchers worldwide to make the most use of published data (Doskey *et al.* 2015).

2.2. Mitochondrial preparations

Mitochondrial preparations are defined as either isolated mitochondria or tissue and cellular preparations in which the barrier function of the plasma membrane is disrupted. Since this entails the loss of cell viability, mitochondrial preparations are not studied *in vivo*. In contrast to isolated mitochondria and tissue homogenate preparations, mitochondria in permeabilized tissues and cells are *in situ* relative to the plasma membrane. When studying mitochondrial preparations, substrate-uncoupler-inhibitor-titration (SUIT) protocols are used to establish respiratory coupling control states (CCS) and pathway control states (PCS) that provide reference values for various output variables (**Table 1**). Physiological conditions *in vivo* deviate from these experimentally obtained states; this is because kinetically-saturating concentrations, *e.g.*, of ADP, oxygen (O_2; dioxygen) or fuel substrates, may not apply to physiological intracellular conditions. Further information is obtained in studies of kinetic responses to variations in fuel substrate concentrations, [ADP], or [O_2] in the range between kinetically-saturating concentrations and anoxia (Gnaiger 2001).

The cholesterol content of the plasma membrane is high compared to mitochondrial membranes (Korn 1969). Therefore, mild detergents—such as digitonin and saponin—can be applied to selectively permeabilize the plasma membrane via interaction with cholesterol; this allows free exchange of organic molecules and inorganic ions between the cytosol and the immediate cell environment, while maintaining the integrity and localization of organelles, cytoskeleton, and the nucleus. Application of permeabilization agents (mild detergents or toxins) leads to washout of cytosolic marker enzymes—such as lactate dehydrogenase—and results in the complete loss of cell viability (tested by nuclear staining using plasma membrane-impermeable dyes), while mitochondrial function remains intact (tested by cytochrome *c* stimulation of respiration). Digitonin concentrations have to be optimized according to cell type, particularly since mitochondria from cancer cells contain significantly higher contents of cholesterol in both membranes (Baggetto and Testa-Perussini, 1990). For example, a dose of digitonin of 8 fmol·cell^{-1} (10 pg·cell^{-1}; 10 µg·10^{-6} cells) is optimal for permeabilization of endothelial cells, and the concentration in the incubation medium has to be adjusted according to the cell concentration (Doerrier *et al.* 2018). Respiration of isolated mitochondria remains unaltered after the addition of low concentrations of digitonin or saponin. In addition to mechanical cell disruption during homogenization of tissue, permeabilization agents may be applied to ensure permeabilization of all cells in tissue homogenates.

Suspensions of cells permeabilized in the respiration chamber and crude tissue homogenates contain all components of the cell at highly dilute concentrations. All mitochondria are retained in chemically-permeabilized mitochondrial preparations and crude tissue homogenates. In the preparation of isolated mitochondria, however, the mitochondria are separated from other cell fractions and purified by differential centrifugation, entailing the loss of mitochondria at typical recoveries ranging from 30% to 80% of total mitochondrial content (Lai *et al.* 2018). Using Percoll or sucrose density gradients to maximize the purity of isolated mitochondria may compromise the mitochondrial yield or structural and functional integrity. Therefore, mitochondrial isolation protocols need to be optimized according to each study. The term *mitochondrial preparation* neither includes living cells, nor submitochondrial particles and further fractionated mitochondrial components.

2.3. Electron transfer pathways

Mitochondrial electron transfer (ET) pathways are fuelled by diffusion and transport of substrates across the mtOM and mtIM. In addition, the mitochondrial electron transfer system (ETS) consists of the matrix-ETS and membrane-ETS (**Figure 2B**). Upstream sections of ET-pathways converge at the NADH-junction (N-junction). NADH is mainly generated in the tricarboxylic acid (TCA) cycle and is oxidized by Complex I (CI), with further electron entry into the coenzyme Q-junction (Q-junction).

Similarly, succinate is formed in the TCA cycle and oxidized by CII to fumarate. CII is part of both the TCA cycle and the ETS, and reduces FAD to $FADH_2$ with further reduction of ubiquinone to ubiquinol downstream of the TCA cycle in the Q-junction. Thus $FADH_2$ is not a substrate but is the product of CII, in contrast to erroneous metabolic maps shown in many publications. β-oxidation of fatty acids (FA) supplies reducing equivalents via (*1*) $FADH_2$ as the substrate of electron transferring flavoprotein complex (CETF); (*2*) acetyl-CoA generated by chain shortening; and (*3*) NADH generated via 3-hydroxyacyl-CoA dehydrogenases. The ATP yield depends on whether acetyl-CoA enters the TCA cycle, or is for example used in ketogenesis.

Selected mitochondrial catabolic pathways, k, of electron transfer from the oxidation of fuel substrates to the reduction of O_2 are stimulated by addition of fuel substrates to the mitochondrial respiration medium after depletion of endogenous substrates (**Figure 2B**). Substrate combinations and specific inhibitors of ET-pathway enzymes are used to obtain defined pathway control states in mitochondrial preparations (Gnaiger 2014).

2.4. Respiratory coupling control

2.4.1. Coupling: In mitochondrial electron transfer, vectorial transmembrane proton flux is coupled through the redox proton pumps CI, CIII and CIV to the catabolic flux of scalar reactions, collectively measured as O_2 flux, J_{kO_2} (**Figure 2**). Thus mitochondria are elementary components of energy transformation. Energy is a conserved quantity and cannot be lost or produced in any internal process (First Law of Thermodynamics). Open and closed systems can gain or lose energy only by external fluxes—by exchange with the environment. Therefore, energy can neither be produced by mitochondria, nor is there any internal process without energy conservation. Exergy or Gibbs energy ('free energy') is the part of energy that can potentially be transformed into work under conditions of constant temperature and pressure. *Coupling* is the interaction of an exergonic process (spontaneous, negative exergy change) with an endergonic process (positive exergy change) in energy transformations which conserve part of the exergy change. Exergy is not completely conserved, however, except at the limit of 100% efficiency of energy transformation in a coupled process. The exergy or Gibbs energy change that is not conserved by copling is irreversibly lost or dissipated, and is accounted for as the entropy change of the surroundings and the system, multiplied by the temperature of the irreversible process.

Pathway control states (PCS) and coupling control states (CCS) are complementary, since mitochondrial preparations depend on (*1*) an exogenous supply of pathway-specific fuel substrates and oxygen, and (*2*) exogenous control of phosphorylation (**Figure 2**).

2.4.2. Phosphorylation, P», and P»/O_2 ratio: Phosphorylation in the context of OXPHOS is defined as phosphorylation of ADP by P_i to form ATP. On the other hand, the term phosphorylation is used generally in many contexts, *e.g.*, protein phosphorylation. This provides the argument for introducing a symbol more discriminating and specific than P as used in the P/O ratio (phosphate to atomic oxygen ratio), where P indicates phosphorylation of ADP to ATP or GDP to GTP (**Figure 2**): The symbol P» indicates the endergonic (uphill) direction of phosphorylation ADP→ATP, and likewise P« the corresponding exergonic (downhill) hydrolysis ATP→ADP. P» refers mainly to electrontransfer phosphorylation but may also involve substrate-level phosphorylation as part of the TCA cycle (succinyl-CoA ligase, phosphoglycerate kinase) and phosphorylation of ADP catalyzed by pyruvate kinase, and of GDP phosphorylated by phosphoenolpyruvate carboxykinase. Transphosphorylation is performed by adenylate kinase, creatine kinase (mtCK), hexokinase and nucleoside diphosphate kinase. In isolated mammalian mitochondria, ATP production catalyzed by adenylate kinase (2 ADP ↔ ATP + AMP) proceeds without fuel substrates in the presence of ADP (Komlódi and Tretter 2017). Kinase cycles are involved in intracellular energy transfer and signal transduction for regulation of energy flux.

The P»/O_2 ratio (P»/4 e^-) is two times the 'P/O' ratio (P»/2 e^-). P»/O_2 is a generalized symbol, not specific for reporting P_i consumption (P_i/O_2 flux ratio), ADP depletion (ADP/O_2 flux ratio), or ATP production (ATP/O_2 flux ratio). The mechanistic P»/O_2 ratio—or P»/O_2 stoichiometry—is calculated from the proton–to–O_2 and proton–to–phosphorylation coupling stoichiometries (**Figure 2B**):

$$\mathrm{P»/O_2} = \frac{\mathrm{H^+_{pos}/O_2}}{\mathrm{H^+_{neg}/P»}} \quad (1)$$

The H^+_{pos}/O_2 coupling stoichiometry (referring to the full four electron reduction of O_2) depends on the relative involvement of the three coupling sites (respiratory Complexes CI, CIII and CIV) in the

catabolic ET-pathway from reduced fuel substrates (electron donors) to the reduction of O_2 (electron acceptor). This varies with: (*1*) a bypass of CI by single or multiple electron input into the Q-junction; and (*2*) a bypass of CIV by involvement of alternative oxidases, AOX. AOX are expressed in all plants, some fungi, many protists, and several animal phyla, but are not expressed in vertebrate mitochondria (McDonald *et al.* 2009).

The H^+_{pos}/O_2 coupling stoichiometry equals 12 in the ET-pathways involving CIII and CIV as proton pumps, increasing to 20 for the NADH-pathway through CI (**Figure 2B**). A general consensus on H^+_{pos}/O_2 stoichiometries, however, remains to be reached (Hinkle 2005; Wikström and Hummer 2012; Sazanov 2015). The H^+_{neg}/P» coupling stoichiometry (3.7; **Figure 2B**) is the sum of 2.7 H^+_{neg} required by the F-ATPase of vertebrate and most invertebrate species (Watt *et al.* 2010) and the proton balance in the translocation of ADP, ATP and P_i (**Figure 2C**). Taken together, the mechanistic P»/O_2 ratio is calculated at 5.4 and 3.3 for the N- and S-pathway, respectively (Eq. 1). The corresponding classical P»/O ratios (referring to the 2 electron reduction of 0.5 O_2) are 2.7 and 1.6 (Watt *et al.* 2010), in agreement with the measured P»/O ratio for succinate of 1.58 ± 0.02 (Gnaiger *et al.* 2000).

2.4.3. Uncoupling: The effective P»/O_2 flux ratio ($Y_{P»/O_2} = J_{P»}/J_{kO_2}$) is diminished relative to the mechanistic P»/O_2 ratio by intrinsic and extrinsic uncoupling or dyscoupling (**Figure 3**). This is distinct from switching between mitochondrial pathways that involve fewer than three proton pumps ('coupling sites': Complexes CI, CIII and CIV), bypassing CI through multiple electron entries into the Q-junction, or bypassing CIII and CIV through AOX (**Figure 2B**). Reprogramming of mitochondrial pathways leading to different types of substrates being oxidized may be considered as a switch of gears (changing the stoichiometry by altering the substrate that is oxidized) rather than uncoupling (loosening the tightness of coupling relative to a fixed stoichiometry). In addition, $Y_{P»/O_2}$ depends on several experimental conditions of flux control, increasing as a hyperbolic function of [ADP] to a maximum value (Gnaiger 2001).

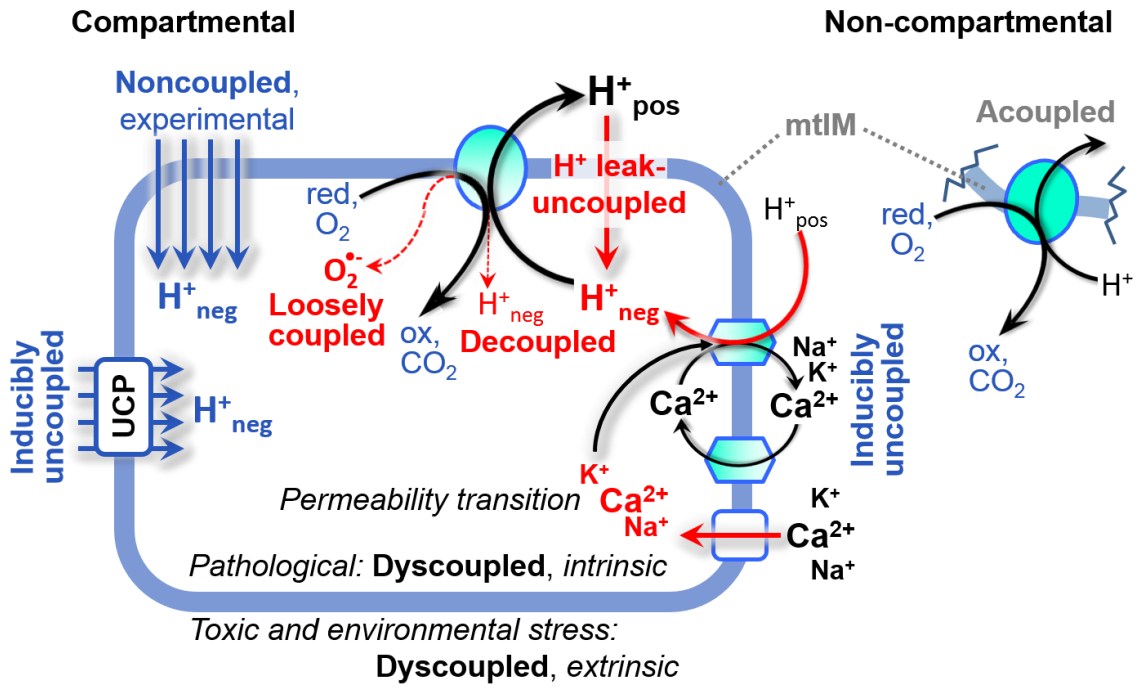

Figure 3. Mechanisms of respiratory uncoupling
An intact mitochondrial inner membrane, mtIM, is required for vectorial, compartmental coupling. Inducible uncoupling, *e.g.*, by activation of UCP1, increases LEAK-respiration; experimentally noncoupled respiration provides an estimate of ET-capacity obtained by titration of protonophores stimulating respiration to maximum O_2 flux. H^+ leak-uncoupled, decoupled, and loosely coupled respiration are components of intrinsic uncoupling (**Table 2**). Pathological dysfunction may affect all types of uncoupling, including permeability transition (mtPT), causing intrinsically dyscoupled respiration. Similarly, toxicological and environmental stress factors can cause extrinsically dyscoupled respiration. 'Acoupled' respiration is the consequence of structural disruption with catalytic activity of non-compartmental mitochondrial fragments. Reduced fuel substrates, red; oxidized products, ox.

Uncoupling of mitochondrial respiration is a general term comprising diverse mechanisms (**Figure 3**):

1. Proton leak across the mtIM from the positive to the negative compartment (H^+ leak-uncoupled)
2. Cycling of other cations, strongly stimulated by mtPT; comparable to the use of protonophores, cation cycling is experimentally induced by valinomycin in the presence of K^+
3. Decoupling by proton slip in the redox proton pumps when protons are effectively not pumped (CI, CIII and CIV) or are not driving phosphorylation (F-ATPase)
4. Loss of vesicular (compartmental) integrity when electron transfer is acoupled
5. Electron leak in the loosely coupled univalent reduction of O_2 to superoxide ($O_2^{\bullet-}$; superoxide anion radical)

Differences of terms—uncoupled *vs.* noncoupled—are easily overlooked, although they relate to different meanings of uncoupling (**Figure 3** and **Table 2**).

2.5. Coupling states and respiratory rates

To extend the classical nomenclature on mitochondrial coupling states (Section 2.6) by a concept-driven terminology that explicitly incorporates information on the meaning of respiratory states, the terminology must be general and not restricted to any particular experimental protocol or mitochondrial preparation (Gnaiger 2009). Concept-driven nomenclature aims at mapping the meaning and concept behind the words and acronyms onto the forms of words and acronyms (Miller 1991). The focus of concept-driven nomenclature is primarily the conceptual *why*, along with clarification of the experimental *how* (**Table 1**).

Table 1. Coupling states and rates, and residual oxygen consumption in mitochondrial preparations. Respiration- and phosphorylation-flux, J_{kO_2} and $J_{P»}$, are rates, characteristic of a state in conjunction with the protonmotive force, pmf. Coupling states are established at kinetically-saturating concentrations of fuel substrates and O_2.

State	Rate	J_{kO_2}	$J_{P»}$	pmf	Inducing factors	Limiting factors
LEAK	*L*	low, cation leak-dependent respiration	0	max.	back-flux of cations including proton leak, proton slip	$J_{P»}$ = 0: (*1*) without ADP, *L*(n); (*2*) max. ATP/ADP ratio, *L*(T); or (*3*) inhibition of the phosphorylation-pathway, *L*(Omy)
OXPHOS	*P*	high, ADP-stimulated respiration, OXPHOS-capacity	max.	high	kinetically-saturating [ADP] and [P_i]	$J_{P»}$ by phosphorylation-pathway capacity; or J_{kO_2} by ET-capacity
ET	*E*	max., noncoupled respiration, ET-capacity	0	low	optimal external uncoupler concentration for max. $J_{O_2,E}$	J_{kO_2} by ET-capacity
ROX	*Rox*	min., residual O_2 consumption	0	0	$J_{O_2,Rox}$ in non-ET-pathway oxidation reactions	inhibition of all ET-pathways; or absence of fuel substrates

To provide a diagnostic reference for respiratory capacities of core energy metabolism, the OXPHOS-capacity is measured at kinetically-saturating concentrations of ADP and P_i. The ET- and phosphorylation-pathways comprise coupled segments of the OXPHOS-system. By application of external uncouplers, ET-capacity is measured as noncoupled respiration. Compared to OXPHOS capacity, the oxidative ET-capacity reveals the limitation of OXPHOS-capacity mediated by the phosphorylation-pathway. The contribution of intrinsically uncoupled O_2 consumption is studied by preventing the stimulation of phosphorylation either in the absence of ADP or by inhibition of the

phosphorylation-pathway. The corresponding states are collectively classified as LEAK-states when O_2 consumption compensates mainly for ion leaks, including the proton leak. Defined coupling states are induced by: (*1*) adding cation chelators such as EGTA, binding free Ca^{2+} and thus limiting cation cycling; (*2*) adding ADP and P_i; (*3*) inhibiting the phosphorylation-pathway; and (*4*) uncoupler titrations, while maintaining a defined ET-pathway state with constant fuel substrates and inhibitors of specific branches of the ET-pathway.

The three coupling states, ET, OXPHOS, and LEAK are shown schematically with the corresponding respiratory rates, abbreviated as *E*, *P*, and *L*, respectively (**Figure 4**). We distinguish metabolic *pathways* from metabolic *states* and the corresponding metabolic *rates*; for example: ET-pathways, ET-states, and ET-capacities, *E*, respectively (**Table 1**). The protonmotive force is *maximum* in the LEAK-state of coupled mitochondria, driven by LEAK-respiration at a minimum back-flux of cations to the matrix side, *high* in the OXPHOS-state when it drives phosphorylation, and *very low* in the ET-state when uncouplers short-circuit the proton cycle (**Table 1**).

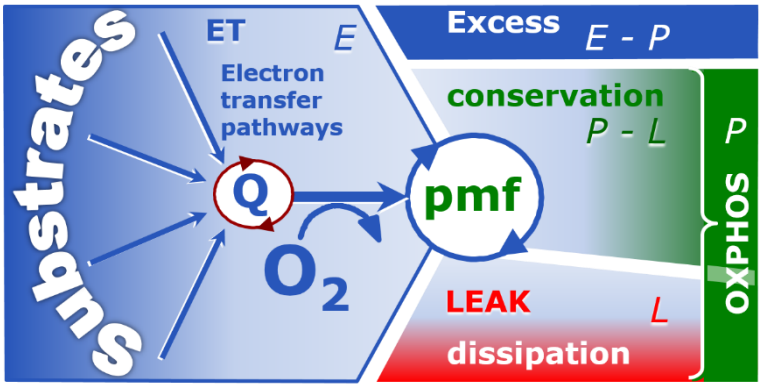

Figure 4. Four-compartment model of oxidative phosphorylation
Respiratory states (ET, OXPHOS, LEAK; **Table 1**) and corresponding rates (*E*, *P*, *L*) are connected by the protonmotive force, pmf. (*1*) ET-capacity, *E*, is partitioned into (*2*) dissipative LEAK-respiration, *L*, when the Gibbs energy change of catabolic O_2 flux is irreversibly lost, (*3*) net OXPHOS-capacity, *P-L*, with partial conservation of the capacity to perform work, and (*4*) the excess capacity, *E-P*. Modified from Gnaiger (2014).

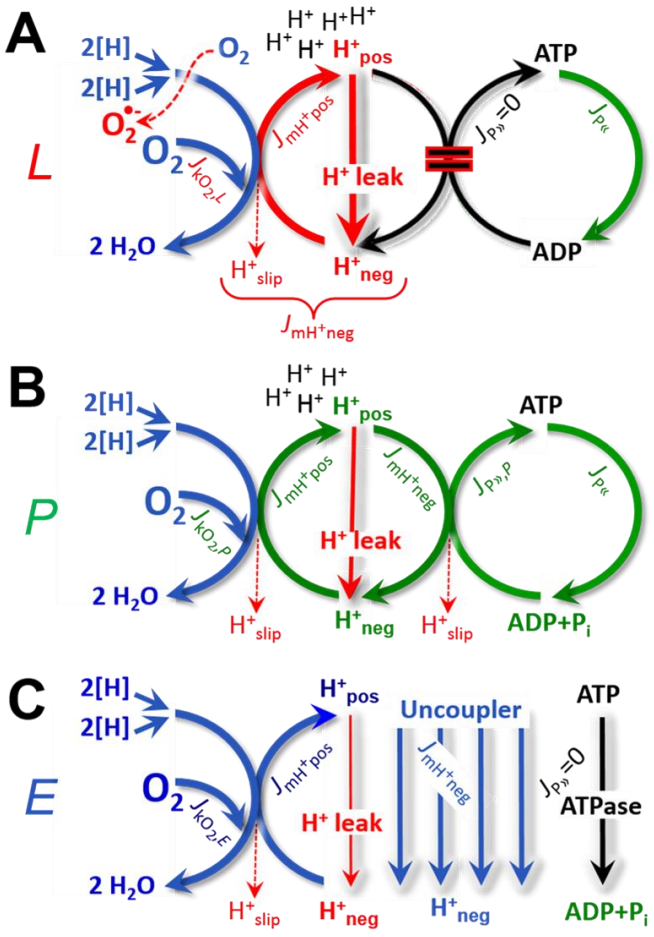

Figure 5. Respiratory coupling states
(A) LEAK-state and rate, *L*: Oxidation only, since phosphorylation is arrested, $J_{P»} = 0$, and catabolic O_2 flux, $J_{kO_2,L}$, is controlled mainly by the proton leak and slip, J_{mH^+neg}, at maximum protonmotive force (**Figure 4**). ATP may be hydrolyzed by ATPases, $J_{P«}$; then phosphorylation must be blocked.
(B) OXPHOS-state and rate, *P*: Oxidation coupled to phosphorylation, $J_{P»}$, which is stimulated by kinetically-saturating [ADP] and [P_i], supported by a high protonmotive force. O_2 flux, $J_{kO_2,P}$, is well-coupled at a P»/O_2 flux ratio of $J_{P»,P} \cdot J_{O_2,P}^{-1}$. Extramitochondrial ATPases may recycle ATP, $J_{P«}$.
(C) ET-state and rate, *E*: Oxidation only, since phosphorylation is zero, $J_{P»} = 0$, at optimum exogenous uncoupler concentration when noncoupled respiration, $J_{kO2,E}$, is maximum. The F-ATPase may hydrolyze extramitochondrial ATP.

2.5.1. LEAK-state (**Figure 5A**): The LEAK-state is defined as a state of mitochondrial respiration when O_2 flux mainly compensates for ion leaks in the absence of ATP synthesis, at kinetically-saturating concentrations of O_2, respiratory fuel substrates and P_i. LEAK-respiration is measured to obtain an estimate of intrinsic uncoupling without addition of an experimental uncoupler: (*1*) in the absence of adenylates, *i.e.*, AMP, ADP and ATP; (*2*) after depletion of ADP at a maximum ATP/ADP ratio; or (*3*) after inhibition of the phosphorylation-pathway by inhibitors of F-ATPase (oligomycin), or adenine nucleotide translocase (carboxyatractyloside). Adjustment of the nominal concentration of these inhibitors to the concentration of biological sample applied can minimize or avoid inhibitory side-effects exerted on ET-capacity or even some dyscoupling.

Table 2. Terms on respiratory coupling and uncoupling.

Term		J_{kO_2}	P»/O_2	Notes
intrinsic, no protonophore added	uncoupled	*L*	0	non-phosphorylating LEAK-respiration (**Figure 5A**)
	proton leak-uncoupled		0	component of *L*, H^+ diffusion across the mtIM (**Figure 3**)
	inducibly uncoupled		0	by UCP1 or cation (*e.g.*, Ca^{2+}) cycling (**Figure 3**)
	decoupled		0	component of *L*, proton slip (**Figure 3**)
	loosely coupled		0	component of *L*, lower coupling due to superoxide formation and bypass of proton pumps by electron leak (**Figure 3**)
	dyscoupled		0	mitochondrial dysfunction due to pathologically, toxicologically, environmentally increased uncoupling
noncoupled		*E*	0	ET-capacity, non-phosphorylating respiration stimulated to maximum flux at optimum exogenous protonophore concentration (**Figure 5C**)
well-coupled		*P*	high	OXPHOS-capacity, phosphorylating respiration with an intrinsic LEAK component (**Figure 5B**)
fully coupled		*P – L*	max.	OXPHOS-capacity corrected for LEAK-respiration (**Figure 4**)
acoupled			0	electron transfer in mitochondrial fragments without vectorial proton translocation (**Figure 3**)

- **Proton leak and uncoupled respiration:** The intrinsic proton leak is the *uncoupled* leak current of protons in which protons diffuse across the mtIM in the dissipative direction of the downhill protonmotive force without coupling to phosphorylation (**Figure 5A**). The proton leak flux depends non-linearly on the protonmotive force (Garlid *et al.* 1989; Divakaruni and Brand 2011), which is a temperature-dependent property of the mtIM and may be enhanced due to possible contamination by free fatty acids. Inducible uncoupling mediated by uncoupling protein 1 (UCP1) is physiologically controlled, *e.g.*, in brown adipose tissue. UCP1 is a member of the mitochondrial carrier family that is involved in the translocation of protons across the mtIM (Jezek *et al.* 2018). Consequently, this short-circuit lowers the protonmotive force and stimulates electron transfer, respiration, and heat dissipation in the absence of phosphorylation of ADP.
- **Cation cycling:** There can be other cation contributors to leak current including calcium and probably magnesium. Calcium influx is balanced by mitochondrial Na^+/Ca^{2+} or H^+/Ca^{2+} exchange, which is balanced by Na^+/H^+ or K^+/H^+ exchanges. This is another effective uncoupling mechanism different from proton leak (**Table 2**).
- **Proton slip and decoupled respiration:** Proton slip is the *decoupled* process in which protons are only partially translocated by a redox proton pump of the ET-pathways and slip back to the original vesicular compartment. The proton leak is the dominant contributor to the overall leak

current in mammalian mitochondria incubated under physiological conditions at 37 °C, whereas proton slip increases at lower experimental temperature (Canton *et al.* 1995). Proton slip can also happen in association with the F-ATPase, in which the proton slips downhill across the pump to the matrix without contributing to ATP synthesis. In each case, proton slip is a property of the proton pump and increases with the pump turnover rate.

- **Electron leak and loosely coupled respiration**: Superoxide production by the ETS leads to a bypass of redox proton pumps and correspondingly lower P»/O_2 ratio. This depends on the actual site of electron leak and the scavenging of hydrogen peroxide by cytochrome *c*, whereby electrons may re-enter the ETS with proton translocation by CIV.
- **Dyscoupled respiration:** Mitochondrial injuries may lead to *dyscoupling* as a pathological or toxicological cause of *uncoupled* respiration. Dyscoupling may involve any type of uncoupling mechanism, *e.g.*, opening the mtPT pore. Dyscoupled respiration is distinguished from experimentally induced *noncoupled* respiration in the ET-state (**Table 2**).
- **Protonophore titration and noncoupled respiration:** Protonophores are uncouplers which are titrated to obtain maximum *noncoupled* respiration as a measure of ET-capacity.
- **Loss of compartmental integrity and acoupled respiration:** Electron transfer and catabolic O_2 flux proceed without compartmental proton translocation in disrupted mitochondrial fragments. Such fragments are an artefact of mitochondrial isolation, and may not fully fuse to re-establish structurally intact mitochondria. Loss of mtIM integrity, therefore, is the cause of acoupled respiration, which is a nonvectorial dissipative process without control by the protonmotive force.

2.5.2. OXPHOS-state (Figure 5B): The OXPHOS-state is defined as the respiratory state with kinetically-saturating concentrations of O_2, respiratory and phosphorylation substrates, and absence of exogenous uncoupler, which provides an estimate of the maximal respiratory capacity in the OXPHOS-state for any given ET-pathway state. Respiratory capacities at kinetically-saturating substrate concentrations provide reference values or upper limits of performance, aiming at the generation of data sets for comparative purposes. Physiological activities and effects of substrate kinetics can be evaluated relative to the OXPHOS-capacity.

As discussed previously, 0.2 mM ADP does not kinetically-saturate flux in isolated mitochondria (Gnaiger 2001; Puchowicz *et al.* 2004); greater [ADP] is required, particularly in permeabilized muscle fibers and cardiomyocytes, to overcome limitations by intracellular diffusion and by the reduced conductance of the mtOM (Jepihhina *et al.* 2011; Illaste *et al.* 2012; Simson *et al*. 2016), either through interaction with tubulin (Rostovtseva *et al.* 2008) or other intracellular structures (Birkedal *et al*. 2014). In addition, kinetically-saturating ADP concentrations need to be evaluated under different experimental conditions such as temperature (Lemieux *et al.* 2017) and with different animal models (Blier and Guderley 1993). In permeabilized muscle fiber bundles of high respiratory capacity, the apparent K_m for ADP increases up to 0.5 mM (Saks *et al.* 1998), consistent with experimental evidence that >90% kinetic saturation is reached only at >5 mM ADP (Pesta and Gnaiger 2012). Similar ADP concentrations are also required for accurate determination of OXPHOS-capacity in human clinical cancer samples and permeabilized cells (Klepinin *et al.* 2016; Koit *et al.* 2017). 2.5 to 5 mM ADP is sufficient to obtain the actual OXPHOS-capacity in many types of permeabilized tissue and cell preparations, but experimental validation is required in each specific case.

2.5.3. Electron transfer-state (Figure 5C): O_2 flux determined in the ET-state yields an estimate of ET-capacity. The ET-state is defined as the *noncoupled* state with kinetically-saturating concentrations of O_2, respiratory substrate and optimum exogenous uncoupler concentration for maximum O_2 flux. Uncouplers are weak lipid-soluble acids which function as protonophores. These disrupt the barrier function of the mtIM and thus short-circuit the protonmotive system, functioning like a clutch in a mechanical system. As a consequence of the nearly collapsed protonmotive force, the driving force is insufficient for phosphorylation, and $J_{P»} = 0$. The most frequently used uncouplers are carbonyl cyanide m-chloro phenyl hydrazone (CCCP), carbonyl cyanide *p*-trifluoromethoxyphenylhydrazone (FCCP), or dinitrophenol (DNP). Stepwise titration of uncouplers stimulates respiration up to or above the level of O_2 consumption rates in the OXPHOS-state; respiration is inhibited, however, above optimum uncoupler concentrations (Mitchell 2011). Data obtained with a single dose of uncoupler must be evaluated with caution, particularly when a fixed uncoupler concentration is used in studies exploring a treatment or disease that may alter the mitochondrial content or mitochondrial sensitivity to inhibition by uncouplers. There is a need for new protonophoric

uncouplers that drive maximal respiration across a broad dosing range and do not inhibit respiration at high concentrations (Kenwood *et al.* 2013). The effect on ET-capacity of the reversed function of F-ATPase ($J_{P«}$; **Figure 5C**) can be evaluated in the presence and absence of extramitochondrial ATP.

2.5.4. ROX state: The state of residual O_2 consumption, ROX, is not a coupling state, but is relevant to assess respiratory function (**Figure 1**). The rate of residual oxygen consumption, *Rox*, is defined as O_2 consumption due to oxidative reactions measured after inhibition of ET with rotenone, malonic acid and antimycin A. Cyanide and azide inhibit not only CIV but catalase and several peroxidases involved in *Rox*. High concentrations of antimycin A, but not rotenone or cyanide, inhibit peroxisomal acyl-CoA oxidase and D-amino acid oxidase (Vamecq *et al.* 1987). *Rox* represents a baseline used to correct respiration measured in defined coupling control states. *Rox*-corrected *L*, *P* and *E* not only lower the values of total fluxes, but also change the flux control ratios *L*/*P* and *L*/*E*. *Rox* is not necessarily equivalent to non-mitochondrial reduction of O_2, considering O_2-consuming reactions in mitochondria that are not related to ET—such as O_2 consumption in reactions catalyzed by monoamine oxidases (type A and B), monooxygenases (cytochrome P450 monooxygenases), dioxygenase (sulfur dioxygenase and trimethyllysine dioxygenase), and several hydoxylases. Isolated mitochondrial fractions, especially those obtained from liver, may be contaminated by peroxisomes, as shown by transmission electron microscopy. This fact makes the exact determination of mitochondrial O_2 consumption and mitochondria-associated generation of reactive oxygen species complicated (Schönfeld *et al.* 2009; Speijer 2016; **Figure 2**). The variability of ROX-linked O_2 consumption needs to be studied in relation to non-ET enzyme activities, availability of specific substrates, O_2 concentration, and electron leakage leading to the formation of reactive oxygen species.

2.5.5. Quantitative relations: *E* may exceed or be equal to *P*. *E* > *P* is observed in many types of mitochondria, varying between species, tissues and cell types (Gnaiger 2009). *E*-*P* is the excess ET-capacity pushing the phosphorylation-flux to the limit of its capacity for utilizing the protonmotive force (**Figure 4**). In addition, the magnitude of *E*-*P* depends on the tightness of respiratory coupling or degree of uncoupling, since an increase of *L* causes *P* to increase towards the limit of *E* (Lemieux *et al.* 2011). The *excess E*-*P* capacity, *E*-*P*, therefore, provides a sensitive diagnostic indicator of specific injuries of the phosphorylation-pathway, under conditions when *E* remains constant but *P* declines relative to controls. Substrate cocktails supporting simultaneous convergent electron transfer to the Q-junction for reconstitution of TCA cycle function establish pathway control states with high ET-capacity, and consequently increase the sensitivity of the *E*-*P* assay.

E cannot theoretically be lower than *P*. *E* < *P* must be discounted as an artefact, which may be caused experimentally by: (*1*) loss of oxidative capacity during the time course of the respirometric assay, since *E* is measured subsequently to *P*; (*2*) using insufficient uncoupler concentrations; (*3*) using high uncoupler concentrations which inhibit ET (Gnaiger 2008); (*4*) high oligomycin concentrations applied for measurement of *L* before titrations of uncoupler, when oligomycin exerts an inhibitory effect on *E*. On the other hand, the excess ET-capacity is overestimated if kinetically non-saturating [ADP] or [P_i] are used. See State 3 in the next section.

The net OXPHOS-capacity is calculated by subtracting *L* from *P* (**Figure 4**). The net P»/O_2 equals P»/(*P*-*L*), wherein the dissipative LEAK component in the OXPHOS-state may be overestimated. This can be avoided by measuring LEAK-respiration in a state when the protonmotive force is adjusted to its slightly lower value in the OXPHOS-state by titration of an ET inhibitor (Divakaruni and Brand 2011). Any turnover-dependent components of proton leak and slip, however, are underestimated under these conditions (Garlid *et al.* 1993). In general, it is inappropriate to use the term *ATP production* or *ATP turnover* for the difference of O_2 flux measured in the OXPHOS and LEAK states. *P*-*L* is the upper limit of OXPHOS-capacity that is freely available for ATP production (corrected for LEAK-respiration) and is fully coupled to phosphorylation with a maximum mechanistic stoichiometry (**Figure 4**).

LEAK-respiration and OXPHOS-capacity depend on (*1*) the tightness of coupling under the influence of the respiratory uncoupling mechanisms (**Figure 3**), and (*2*) the coupling stoichiometry, which varies as a function of the substrate type undergoing oxidation in ET-pathways with either two or three coupling sites (**Figure 2B**). When substrate cocktails are used supporting the convergent NADH- and succinate-pathways simultaneously, the relative contribution of ET-pathways with three or two coupling sites cannot be controlled experimentally, is difficult to determine, and may shift in transitions between LEAK-, OXPHOS- and ET-states (Gnaiger 2014). Under these experimental conditions, we cannot separate the tightness of coupling *versus* coupling stoichiometry as the mechanisms of respiratory control in a shift of *L*/*P* ratios. The tightness of coupling and fully coupled

O_2 flux, *P-L* (**Table 2**), therefore, are obtained from measurements of coupling control of LEAK-respiration, OXPHOS- and ET-capacities in well-defined pathway states, using either pyruvate and malate as substrates or the classical succinate and rotenone substrate-inhibitor combination (**Figure 2B**).

2.5.6. The steady-state: Mitochondria represent a thermodynamically open system in non-equilibrium states of biochemical energy transformation. State variables (protonmotive force; redox states) and metabolic *rates* (fluxes) are measured in defined mitochondrial respiratory *states*. Steady-states can be obtained only in open systems, in which changes by internal transformations, *e.g.*, O_2 consumption, are instantaneously compensated for by external fluxes across the system boundary, *e.g.*, O_2 supply, preventing a change of O_2 concentration in the system (Gnaiger 1993b). Mitochondrial respiratory states monitored in closed systems satisfy the criteria of pseudo-steady states for limited periods of time, when changes in the system (concentrations of O_2, fuel substrates, ADP, P_i, H^+) do not exert significant effects on metabolic fluxes (respiration, phosphorylation). Such pseudo-steady states require respiratory media with sufficient buffering capacity and substrates maintained at kinetically-saturating concentrations, and thus depend on the kinetics of the processes under investigation.

2.6. Classical terminology for isolated mitochondria

> *'When a code is familiar enough, it ceases appearing like a code; one forgets that there is a decoding mechanism. The message is identical with its meaning'* (Hofstadter 1979).

Chance and Williams (1955; 1956) introduced five classical states of mitochondrial respiration and cytochrome redox states. **Table 3** shows a protocol with isolated mitochondria in a closed respirometric chamber, defining a sequence of respiratory states. States and rates are not distinguished in this nomenclature.

Table 3. Metabolic states of mitochondria (Chance and Williams, 1956; Table V).

State	[O_2]	ADP level	Substrate level	Respiration rate	Rate-limiting substance
1	>0	low	low	slow	ADP
2	>0	high	~0	slow	substrate
3	>0	high	high	fast	respiratory chain
4	>0	low	high	slow	ADP
5	0	high	high	0	oxygen

2.6.1. State 1 is obtained after addition of isolated mitochondria to air-saturated isoosmotic/isotonic respiration medium containing P_i, but no fuel substrates and no adenylates.

2.6.2. State 2 is induced by addition of a 'high' concentration of ADP (typically 100 to 300 µM), which stimulates respiration transiently on the basis of endogenous fuel substrates and phosphorylates only a small portion of the added ADP. State 2 is then obtained at a low respiratory activity limited by exhausted endogenous fuel substrate availability (**Table 3**). If addition of specific inhibitors of respiratory complexes such as rotenone does not cause a further decline of O_2 flux, State 2 is equivalent to the ROX state (**Table 1**). Undefined endogenous fuel substrates are a confounding factor of pathway control, contributing to the effect of subsequently externally added substrates and inhibitors. In an alternative sequence of titration steps, the second state is induced by addition of fuel substrate without ADP or ATP (Estabrook 1967). In contrast to the original State 2 defined in **Table 1** as a ROX state, the alternative 'State 2' is a LEAK-state with *L*(n). Some researchers have called this condition as 'pseudostate 4'.

2.6.3. State 3 is the state stimulated by addition of fuel substrates while the ADP concentration in the original State 2 is still high (**Table 3**) and supports coupled energy transformation. 'High ADP' is a concentration of ADP specifically selected to allow the measurement of State 3 to State 4 transitions of isolated mitochondria in a closed respirometric chamber. Repeated ADP titration re-establishes State 3 at 'high ADP'. Starting at O_2 concentrations near air-saturation (193 or 238 µM O_2 at 37 °C or 25 °C and sea level at 1 atm or 101.32 kPa, and an oxygen solubility of respiration medium at 0.92 times that of pure water; Forstner and Gnaiger 1983), the total ADP concentration added must be low enough

(typically 100 to 300 µM) to allow phosphorylation to ATP at a coupled O_2 flux that does not lead to O_2 depletion during the transition to State 4. In contrast, kinetically-saturating ADP concentrations usually are 10-fold higher than 'high ADP', *e.g.*, 2.5 mM in isolated mitochondria. The abbreviation State 3u is occasionally used in bioenergetics, to indicate the state of respiration after titration of an uncoupler, without sufficient emphasis on the fundamental difference between OXPHOS-capacity (*well-coupled* with an endogenous uncoupled component) and ET-capacity (*noncoupled*).

2.6.4. State 4 is a LEAK-state that is obtained only if the mitochondrial preparation is intact and well-coupled. Depletion of ADP by phosphorylation to ATP causes a decline of O_2 flux in the transition from State 3 to State 4. Under the conditions of State 4, a maximum protonmotive force and high ATP/ADP ratio are maintained. The gradual decline of $Y_{P»/O_2}$ towards diminishing [ADP] at State 4 must be taken into account for calculation of P»/O_2 ratios (Gnaiger 2001). State 4 respiration, L(T) (**Table 1**), reflects intrinsic proton leak and ATP hydrolysis activity. O_2 flux in State 4 is an overestimation of LEAK-respiration if the contaminating ATP hydrolysis activity recycles some ATP to ADP, $J_{P«}$, which stimulates respiration coupled to phosphorylation, $J_{P»} > 0$. Some degree of mechanical disruption and loss of mitochondrial integrity allows the exposed mitochondrial F-ATPases to hydrolyze the ATP synthesized by the fraction of coupled mitochondria. This can be tested by inhibition of the phosphorylation-pathway using oligomycin, ensuring that $J_{P»} = 0$ (State 4o). On the other hand, the State 4 respiration reached after exhaustion of added ADP is a more physiological condition, *i.e.*, presence of ATP, ADP and even AMP. Sequential ADP titrations re-establish State 3, followed by State 3 to State 4 transitions while sufficient O_2 is available. Anoxia may be reached, however, before exhaustion of ADP (State 5).

2.6.5. State 5 '*may be obtained by antimycin A treatment or by anaerobiosis*' (Chance and Williams, 1955). These definitions give State 5 two different meanings: ROX or anoxia. Anoxia is obtained after exhaustion of O_2 in a closed respirometric chamber. Diffusion of O_2 from the surroundings into the aqueous solution may be a confounding factor preventing complete anoxia (Gnaiger 2001).

In **Table 3**, only States 3 and 4 are coupling control states, with the restriction that rates in State 3 may be limited kinetically by non-saturating ADP concentrations.

2.7. Control and regulation

The terms metabolic *control* and *regulation* are frequently used synonymously, but are distinguished in metabolic control analysis: "We could understand the regulation as the mechanism that occurs when a system maintains some variable constant over time, in spite of fluctuations in external conditions (homeostasis of the internal state). On the other hand, metabolic control is the power to change the state of the metabolism in response to an external signal" (Fell 1997). Respiratory control may be induced by experimental control signals that exert an influence on: (*1*) ATP demand and ADP phosphorylation-rate; (*2*) fuel substrate composition, pathway competition; (*3*) available amounts of substrates and O_2, *e.g.*, starvation and hypoxia; (*4*) the protonmotive force, redox states, flux–force relationships, coupling and efficiency; (*5*) Ca^{2+} and other ions including H^+; (*6*) inhibitors, *e.g.*, nitric oxide or intermediary metabolites such as oxaloacetate; (*7*) signalling pathways and regulatory proteins, *e.g.*, insulin resistance, transcription factor hypoxia inducible factor 1.

Mechanisms of respiratory control and regulation include adjustments of: (*1*) enzyme activities by allosteric mechanisms and phosphorylation; (*2*) enzyme content, concentrations of cofactors and conserved moieties such as adenylates, nicotinamide adenine dinucleotide [NAD^+/NADH], coenzyme Q, cytochrome *c*; (*3*) metabolic channeling by supercomplexes; and *(4)* mitochondrial density (enzyme concentrations) and morphology (membrane area, cristae folding, fission and fusion). Mitochondria are targeted directly by hormones, *e.g.*, progesterone and glucacorticoids, which affect their energy metabolism (Lee *et al.* 2013; Gerö and Szabo 2016; Price and Dai 2016; Moreno *et al.* 2017; Singh *et al*. 2018). Evolutionary or acquired differences in the genetic and epigenetic basis of mitochondrial function (or dysfunction) between individuals; age; biological sex, and hormone concentrations; life style including exercise and nutrition; and environmental issues including thermal, atmospheric, toxic and pharmacological factors, exert an influence on all control mechanisms listed above. For reviews, see Brown 1992; Gnaiger 1993a, 2009; 2014; Paradies *et al.* 2014; Morrow *et al*. 2017.

Lack of control by a metabolic pathway, *e.g.*, phosphorylation-pathway, means that there will be no response to a variable activating it, *e.g.*, [ADP]. The reverse, however, is not true as the absence of a response to [ADP] does not exclude the phosphorylation-pathway from having some degree of

control. The degree of control of a component of the OXPHOS-pathway on an output variable, such as O_2 flux, will in general be different from the degree of control on other outputs, such as phosphorylation-flux or proton leak flux. Therefore, it is necessary to be specific as to which input and output are under consideration (Fell 1997).

Respiratory control refers to the ability of mitochondria to adjust O_2 flux in response to external control signals by engaging various mechanisms of control and regulation. Respiratory control is monitored in a mitochondrial preparation under conditions defined as respiratory states, preferentially under near-physiological conditions of temperature, pH, and medium ionic composition, to generate data of higher biological relevance. When phosphorylation of ADP to ATP is stimulated or depressed, an increase or decrease is observed in electron transfer measured as O_2 flux in respiratory coupling states of intact mitochondria ('controlled states' in the classical terminology of bioenergetics). Alternatively, coupling of electron transfer with phosphorylation is diminished by uncouplers. The corresponding coupling control state is characterized by a high respiratory rate without control by P» (noncoupled or 'uncontrolled state').

3. What is a rate?

The term *rate* is not adequately defined to be useful for reporting data. Normalization of rates leads to a diversity of formats. Application of common and defined units is required for direct transfer of reported results into a database. The second [s] is the SI unit for the base quantity *time*. It is also the standard time-unit used in solution chemical kinetics.

The inconsistency of the meanings of rate becomes apparent when considering Galileo Galilei's famous principle, that 'bodies of different weight all fall at the same rate (have a constant acceleration)' (Coopersmith 2010). A rate may be an extensive quantity, which is a *flow*, *I*, when expressed per *object* (per number of cells or organisms) or per chamber (per instrumental system). *System* is defined as the open or closed chamber of the measuring device. A rate is a *flux*, *J*, when expressed as a size-specific quantity (**Figure 6A; Box 2**).

- **Extensive quantities:** An extensive quantity increases proportionally with system size. For example, mass and volume are extensive quantities. Flow is an extensive quantity. The magnitude of an extensive quantity is completely additive for non-interacting subsystems. The magnitude of these quantities depends on the extent or size of the system (Cohen *et al.* 2008).
- **Size-specific quantities:** 'The adjective *specific* before the name of an extensive quantity is often used to mean *divided by mass*' (Cohen *et al.* 2008). The term *specific* has different meanings in three particular contexts: (*1*) In the system-paradigm, (*a*) mass-specific flux is flow divided by mass of the system (the mass of everything contained in the instrumental chamber or reactor). (*b*) Rates are frequently expressed as volume-specific flux (volume of the instrumental chamber). A mass-specific or volume-specific quantity is independent of the extent of non-interacting homogenous subsystems. (*2*) In the context of *sample size*, tissue-specific quantities are related to the mass or volume of the sample in contrast to the mass or volume of the *system* (*e.g.*, muscle mass-specific or cell volume-specific normalization; **Figure 6**). (*3*) An entirely different meaning is implied in the context of *sample type* (*e.g.*, muscle-specific compared to brain-specific properties).
- **Intensive quantities:** In contrast to size-specific properties, forces are intensive quantities defined as the change of an extensive quantity per advancement of an energy transformation (Gnaiger 1993b).
- **Formats:** The quantity of a sample *X* can be expressed in different formats. n_X, N_X, and m_X are the molar amount, number, and mass of *X*, respectively. When different formats are indicated in symbols of derived quantities, the format ($\underline{n}$, $\underline{N}$, $\underline{m}$) is shown as a subscript (*underlined italic*), such as in $I_{O_2/\underline{N}X}$ and $J_{O_2/\underline{m}X}$. As of 2019 May 20, the definition of the SI unit mole [mol] is based on a natural constant, namely Avogadro's constant: one mole contains exactly $6.02214076 \cdot 10^{23}$ elementary entities, in contrast to the former definition in terms of the number of atoms in the mass of 0.012 kilogram of carbon 12 (Gibney 2018). Metabolic oxygen flow and flux are expressed in the molar format, n_{O_2} [mol], but in the volume format, V_{O_2} [m^3], in ergometry. These formats are distinguished as $J_{\underline{n}O_2/\underline{m}X}$ and $J_{\underline{V}O_2/\underline{m}X}$, respectively, for mass-specific flux. Further examples are given in **Figure 6** and **Table 4**.

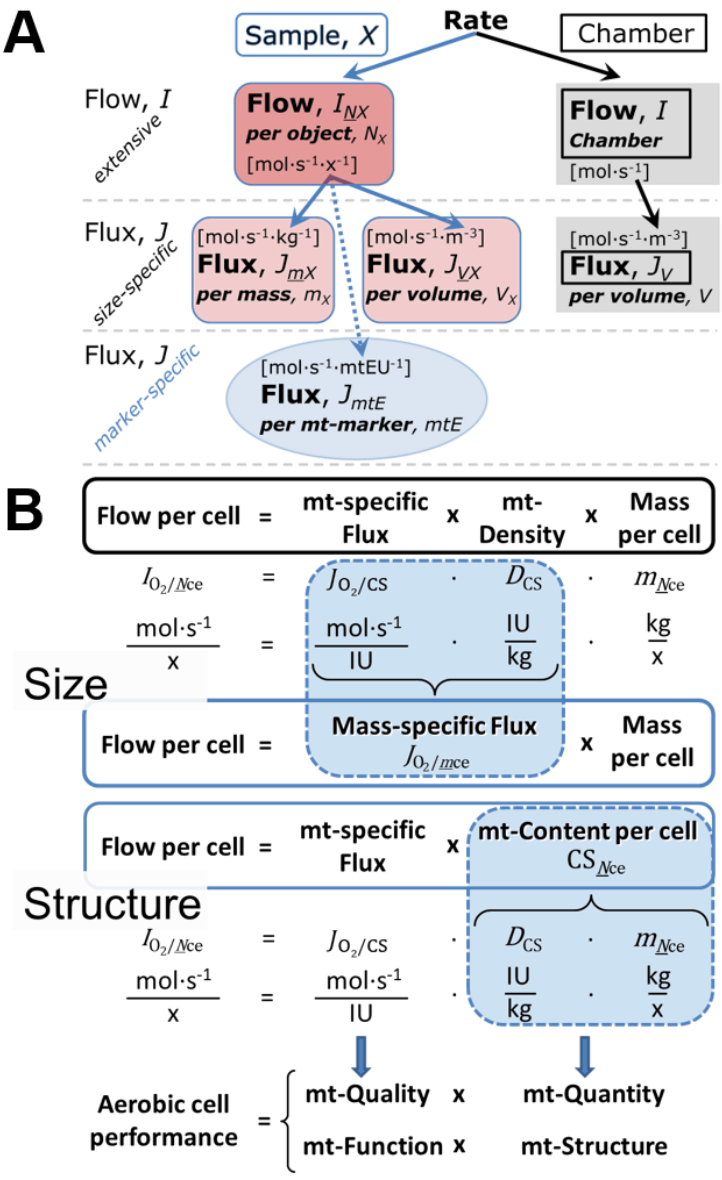

Figure 6. Flow and flux, and normalization in structure-function analysis
(A) A fundamental distinction is made between metabolic rate related to the experimental sample (left) or to the instrumental chamber (right). The different meanings of rate need to be specified by the type of normalization. Left: Results are expressed as mass-specific *flux*, J_{mX}, per mg protein, dry or wet mass. Cell volume, V_{ce}, may be used for normalization (volume-specific flux, J_{Vce}). Right: Flow per instrumental chamber, I, or flux per chamber volume, J_V, are merely reported for methodological reasons. **(B)** O_2 flow per cell, $I_{O2/Nce}$, is the product of mitochondria-specific flux, mt-density and mass per cell. Unstructured analysis: performance is the product of mass-specific flux, $J_{O2/mce}$ [mol·s^{-1}·kg^{-1}], and *size* (mass per cell). Structured analysis: performance is the product of mitochondrial *function* (mt-specific flux) and *structure* (mt-content). Modified from Gnaiger (2014). For further details see **Table 4**.

Box 2: Metabolic flows and fluxes: vectoral, vectorial, and scalar

Flow is an extensive quantity (I; per system), distinguished from flux as a size-specific quantity (J; per system size). *Flows*, I_{tr}, are defined for all transformations as extensive quantities. This is a generalization derived from electrical terms: Electric charge per unit time is electric flow or current, $I_{el} = dQ_{el} \cdot dt^{-1}$ [A≡ C·s^{-1}]. When dividing I_{el} by size of the system (cross-sectional area of a 'wire'), we obtain flux as a size-specific quantity; this is the current density (surface-density of flow) perpendicular to the direction of flux, $\boldsymbol{J}_{el} = I_{el} \cdot A^{-1}$ [A·m^{-2}] (Cohen *et al.* 2008). Fluxes with *spatial* geometric direction and magnitude are *vectors*. Vector and scalar *fluxes* are related to flows as $\boldsymbol{J}_{tr} = I_{tr} \cdot A^{-1}$ [mol·s^{-1}·m^{-2}] and $J_{tr} = I_{tr} \cdot V^{-1}$ [mol·s^{-1}·m^{-3}], expressing flux as an area-specific vector or volume-specific vectorial or scalar quantity, respectively (Gnaiger 1993b). We use the metre–kilogram–second–ampere (MKSA) international system of units (SI) for general cases ([m], [kg], [s] and [A]), with decimal SI prefixes for specific applications (**Table 4**).

We suggest defining: (*1*) *vectoral* fluxes, which are translocations as functions of *gradients* with direction in geometric space in continuous systems; (*2*) *vectorial* fluxes, which describe translocations in discontinuous systems and are restricted to information on *compartmental differences* (transmembrane proton flux); and (*3*) *scalar* fluxes, which are localized transformations without translocation, such as chemical reactions in a homogenous system (catabolic O_2 flux, J_{kO_2}).

4. Normalization of rate per sample

The challenges of measuring mitochondrial respiratory flux are matched by those of normalization. Normalization (**Table 4**) is guided by physicochemical principles, methodological considerations, and conceptual strategies (**Figure 6**).

Table 4. Sample concentrations and normalization of flux.

Expression	Symbol	Definition	Unit	Notes
Sample				
identity of sample	X	object: cell, tissue, animal, patient		
number of sample entities X	N_X	number of objects	x	1
mass of sample X	m_X		kg	2
mass of object X	$m_{\underline{N}X}$	$m_{\underline{N}X} = m_X \cdot N_X^{-1}$	$kg \cdot x^{-1}$	2
Mitochondria				
mitochondria	mt	X = mt		
amount of mt-elementary components	mtE	quantity of mt-marker	mtEU	
Concentrations				
object number concentration	$C_{\underline{N}X}$	$C_{\underline{N}X} = N_X \cdot V^{-1}$	$x \cdot m^{-3}$	3
sample mass concentration	$C_{\underline{m}X}$	$C_{\underline{m}X} = m_X \cdot V^{-1}$	$kg \cdot m^{-3}$	
mitochondrial concentration	C_{mtE}	$C_{mtE} = mtE \cdot V^{-1}$	$mtEU \cdot m^{-3}$	4
specific mitochondrial density	D_{mtE}	$D_{mtE} = mtE \cdot m_X^{-1}$	$mtEU \cdot kg^{-1}$	5
mitochondrial content, mtE per object X	$mtE_{\underline{N}X}$	$mtE_{\underline{N}X} = mtE \cdot N_X^{-1}$	$mtEU \cdot x^{-1}$	6
O_2 flow and flux				7
flow, system	I_{O_2}	internal flow	$mol \cdot s^{-1}$	8
volume-specific flux	J_{V,O_2}	$J_{V,O_2} = I_{O_2} \cdot V^{-1}$	$mol \cdot s^{-1} \cdot m^{-3}$	9
flow per object X	$I_{O_2/\underline{N}X}$	$I_{O_2/\underline{N}X} = J_{V,O_2} \cdot C_{\underline{N}X}^{-1}$	$mol \cdot s^{-1} \cdot x^{-1}$	10
mass-specific flux	$J_{O_2/\underline{m}X}$	$J_{O_2/\underline{m}X} = J_{V,O_2} \cdot C_{\underline{m}X}^{-1}$	$mol \cdot s^{-1} \cdot kg^{-1}$	
mt-marker-specific flux	$J_{O_2/mtE}$	$J_{O_2/mtE} = J_{V,O_2} \cdot C_{mtE}^{-1}$	$mol \cdot s^{-1} \cdot mtEU^{-1}$	11

1 The unit x for a number is not used by IUPAC. To avoid confusion, the units [$kg \cdot x^{-1}$] and [kg] distinguish the mass per object from the mass of a sample that may contain any number of objects. Similarly, the units for flow per system *versus* flow per object are [$mol \cdot s^{-1}$] (Note 8) and [$mol \cdot s^{-1} \cdot x^{-1}$] (Note 10).

2 Units are given in the MKSA system (**Box 2**). The SI prefix k is used for the SI base unit of mass (kg = 1,000 g). In praxis, various SI prefixes are used for convenience, to make numbers easily readable, *e.g.,* 1 mg tissue, cell or mitochondrial mass instead of 0.000001 kg.

3 In case of cells (sample X = cells), the object number concentration is $C_{\underline{N}ce} = N_{ce} \cdot V^{-1}$, and volume may be expressed in [$dm^3 \equiv L$] or [$cm^3 = mL$]. See **Table 5** for different object types.

4 mt-concentration is an experimental variable, dependent on sample concentration: (*1*) $C_{mtE} = mtE \cdot V^{-1}$; (*2*) $C_{mtE} = mtE_X \cdot C_{\underline{N}X}$; (*3*) $C_{mtE} = C_{\underline{m}X} \cdot D_{mtE}$.

5 If the amount of mitochondria, mtE, is expressed as mitochondrial mass, then D_{mtE} is the mass fraction of mitochondria in the sample. If mtE is expressed as mitochondrial volume, V_{mt}, and the mass of sample, m_X, is replaced by volume of sample, V_X, then D_{mtE} is the volume fraction of mitochondria in the sample.

6 $mtE_{\underline{N}X} = mtE \cdot N_X^{-1} = C_{mtE} \cdot C_{\underline{N}X}^{-1}$.

7 O_2 can be replaced by other chemicals to study different reactions, *e.g.,* ATP, H_2O_2, or vesicular compartmental translocations, *e.g.,* Ca^{2+}.

8 I_{O_2} and V are defined per instrumental chamber as a system of constant volume (and constant temperature), which may be closed or open. I_{O_2} is abbreviated for I_{rO_2}, *i.e.*, the metabolic or internal O_2 flow of the chemical reaction r in which O_2 is consumed, hence the negative stoichiometric number, $\nu_{O_2} = -1$. $I_{rO_2} = d_r n_{O_2}/dt \cdot \nu_{O_2}^{-1}$. If r includes all chemical reactions in which O_2 participates, then $d_r n_{O_2} = dn_{O_2} - d_e n_{O_2}$, where dn_{O_2} is the change in the amount of O_2 in the instrumental chamber and $d_e n_{O_2}$ is the amount of O_2 added externally to the system. At steady state, by definition $dn_{O_2} = 0$, hence $d_r n_{O_2} = -d_e n_{O_2}$. Note that in this context 'external', e, refers to the instrumental system, whereas in Figure 1 'external', ext, refers to the organism.

9 J_{V,O_2} is an experimental variable, expressed per volume of the instrumental chamber.

10 $I_{O_2/\underline{N}X}$ is a physiological variable, depending on the size of entity X.

11 There are many ways to normalize for a mitochondrial marker, that are used in different experimental approaches: (*1*) $J_{O_2/mtE} = J_{V,O_2} \cdot C_{mtE}^{-1}$; (*2*) $J_{O_2/mtE} = J_{V,O_2} \cdot C_{\underline{m}X}^{-1} \cdot D_{mtE}^{-1} = J_{O_2/\underline{m}X} \cdot D_{mtE}^{-1}$; (*3*) $J_{O_2/mtE} = J_{V,O_2} \cdot C_{\underline{N}X}^{-1} \cdot mtE_{\underline{N}X}^{-1} = I_{O_2/\underline{N}X} \cdot mtE_{\underline{N}X}^{-1}$; (*4*) $J_{O_2/mtE} = I_{O_2} \cdot mtE^{-1}$. The mt-elementary unit [mtEU] varies depending on the mt-marker.

Table 5. Sample types, *X*, abbreviations, and quantification.

Identity of sample	X	N_X	**Mass**[a]		**Volume**		**mt-Marker**
mitochondrial preparation		[x]	[kg]	[kg·x^{-1}]	[m^3]	[m^3·x^{-1}]	[mtEU]
isolated mitochondria	imt		m_{mt}		V_{mt}		mtE
tissue homogenate	thom		m_{thom}				mtE_{thom}
permeabilized tissue	pti		m_{pti}				mtE_{pti}
permeabilized fiber	pfi		m_{pfi}				mtE_{pfi}
permeabilized cell	pce	N_{pce}	m_{pce}	$m_{\underline{N}pce}$	V_{pce}	$V_{\underline{N}pce}$	mtE_{pce}
living cells[b]	ce	N_{ce}	m_{ce}	$m_{\underline{N}ce}$	V_{ce}	$V_{\underline{N}ce}$	mtE_{ce}
viable cell	vce	N_{vce}	m_{vce}	$m_{\underline{N}vce}$	V_{vce}	$V_{\underline{N}vce}$	
dead cell	dce	N_{dce}	m_{dce}	$m_{\underline{N}dce}$	V_{dce}	$V_{\underline{N}dce}$	
organism	org	N_{org}	m_{org}	$m_{\underline{N}org}$	V_{org}	$V_{\underline{N}org}$	

[a] Instead of mass, the wet weight or dry weight is frequently stated, W_w or W_d. m_X is mass of the sample [kg], $m_{\underline{N}X}$ is mass of the object [kg·x^{-1}] (**Table 4**).

[b] Total cell count in a living cell population, which consists of viable and dead cells, $N_{ce} = N_{vce} + N_{dce}$, without experimental permeabilization of the plasma membrane (sometimes called 'intact' cells in contrast to permeabilized cells).

4.1. Flow: per object

4.1.1. Number concentration, $C_{\underline{N}X}$: Normalization per sample concentration is routinely required to report respiratory data. $C_{\underline{N}X}$ is the experimental number concentration of sample X. In the case of animals N_X is the number of organisms in the chamber, *e.g.*, nematodes, $C_{\underline{N}X} = N_X \cdot V^{-1}$ [x·L^{-1}]. Similarly, the number of cells per chamber volume is the number concentration of cells, $C_{\underline{N}ce} = N_{ce} \cdot V^{-1}$ [x·L^{-1}], where N_{ce} is the number of cells in the chamber (**Table 4**).

4.1.2. Flow per object, $I_{O_2/\underline{N}X}$: O_2 flow per cell is calculated from volume-specific O_2 flux, J_{V,O_2} [nmol·s^{-1}·L^{-1}] (per V of the instrumental chamber [L]), divided by the number concentration of cells. The total cell count is the sum of viable and dead cells, $N_{ce} = N_{vce} + N_{dce}$ (**Table 5**). The cell viability index, $VI = N_{vce} \cdot N_{ce}^{-1}$, is the ratio of the number of viable cells, N_{vce}, per total number of living cells in the population. After experimental permeabilization, all cells are permeabilized, $N_{pce} = N_{ce}$. The cell viability index can be used to normalize respiration for the number of cells that have been viable before experimental permeabilization, $I_{O_2/\underline{N}vce} = I_{O_2/\underline{N}ce} \cdot VI^{-1}$, considering that mitochondrial respiratory dysfunction in dead cells should be eliminated as a confounding factor.

4.2. Size-specific flux: per sample size

4.2.1. Sample concentration, $C_{\underline{m}X}$: Considering permeabilized tissue, homogenate or cells as the sample, X, the sample mass is m_X [mg], which is frequently measured as wet or dry weight, W_w or W_d [mg], respectively, or as mass of protein, $m_{Protein}$. The sample concentration is the mass of the subsample per volume of the instrumental chamber, $C_{\underline{m}X} = m_X \cdot V^{-1}$ [g·L^{-1} = mg·mL^{-1}]. X is the type of sample—isolated mitochondria, tissue homogenate, permeabilized fibers or cells (**Table 4**). m_{ce} [mg] is the total

mass of all cells in an instrumental chamber, whereas $m_{\underline{N}ce} = m_{ce} \cdot N_{ce}^{-1}$ [mg·x^{-1}] is the (average) mass of an individual cell (**Table 5**).

4.2.2. Size-specific flux: Cellular O_2 flow can be compared between cells of identical size. To take into account changes and differences in cell size (Renner *et al.* 2003), normalization is required to obtain cell size-specific or mitochondrial marker-specific O_2 flux (**Figure 6**).

- **Mass-specific flux, $J_{O_2/\underline{m}X}$** [mol·s^{-1}·kg^{-1}]: Mass-specific flux is the expression of respiration per mass of sample, m_X [mg]. Chamber volume-specific flux, J_{V,O_2}, is divided by mass concentration of X in the chamber, $J_{O_2/\underline{m}X} = J_{V,O_2} \cdot C_{\underline{m}X}^{-1}$. Cell mass-specific flux is obtained by dividing flow per cell by mass per cell, $J_{O_2/\underline{m}ce} = I_{O_2/\underline{N}ce} \cdot m_{\underline{N}ce}^{-1}$.
- **Cell volume-specific flux**, $J_{O_2/\underline{V}X}$ [mol·s^{-1}·m^{-3}]: Sample volume-specific flux is obtained by expressing respiration per volume of sample.

If size-specific O_2 flux is constant and independent of sample size, then there is no interaction between the subsystems. For example, 1.5 mg and 3.0 mg sub-samples of muscle tissue respire at identical mass-specific flux. If mass-specific O_2 flux, however, changes as a function of the mass of a tissue sample, cells or isolated mitochondria in the instrumental chamber, then the nature of the interaction becomes an issue. Therefore, cell concentration must be optimized, particularly in experiments carried out in wells, considering the confluency of the cell monolayer or clumps of cells (Salabei *et al.* 2014).

The complexity changes when considering the scaling law of respiratory physiology. Strong interactions are revealed between O_2 flow and body mass of an individual organism: *basal* metabolic rate (flow) does not increase linearly with body mass, whereas *maximum* mass-specific O_2 flux, $\dot{V}_{O2max}$ or $\dot{V}_{O2peak}$, is approximately constant across a large range of individual body mass (Weibel and Hoppeler 2005). Individuals, breeds and species, however, deviate substantially from this relationship. $\dot{V}_{O2peak}$ of human endurance athletes is 60 to 80 mL O_2·min^{-1}·kg^{-1} body mass, converted to $J_{O_2peak/\underline{mN}org}$ of 45 to 60 nmol·s^{-1}·g^{-1} (Gnaiger 2014; **Table 6**).

4.3. Marker-specific flux: per mitochondrial content

Tissues can contain multiple cell populations that may have distinct mitochondrial subtypes. Mitochondria undergo dynamic fission and fusion cycles, and can exist in multiple stages and sizes that may be altered by a range of factors. The isolation of mitochondria (often achieved through differential centrifugation) can therefore yield a subsample of the mitochondrial types present in a tissue, depending on the isolation protocols utilized. This possible bias should be taken into account when planning experiments using isolated mitochondria. Different sizes of mitochondria are enriched at specific centrifugation speeds, which can be used strategically for isolation of mitochondrial subpopulations.

Part of the mitochondrial content of a tissue is lost during preparation of isolated mitochondria. The fraction of isolated mitochondria obtained from a tissue sample is expressed as mitochondrial recovery. At a high mitochondrial recovery, the fraction of isolated mitochondria is more representative of the total mitochondrial population than in preparations characterized by low recovery. Determination of the mitochondrial recovery and yield is based on measurement of the concentration of a mitochondrial marker in the stock suspension of isolated mitochondria, $C_{mtE,stock}$, and crude tissue homogenate, $C_{mtE,thom}$, which together provide information on the specific mitochondrial density in the sample, D_{mtE} (**Table 4**).

When discussing concepts of normalization, it is essential to consider the question posed by the study. If the study aims at comparing tissue performance—such as the effects of a treatment on a specific tissue, then normalization for tissue mass or protein content is appropriate. However, if the aim is to find differences in mitochondrial function independent of mitochondrial density (**Table 4**), then normalization to a mitochondrial marker is imperative (**Figure 6**). One cannot assume that quantitative changes in various markers—such as mitochondrial proteins—necessarily occur in parallel with one another. It should be established that the marker chosen is not selectively altered by the performed treatment. In conclusion, the normalization must reflect the question under investigation to reach a satisfying answer. On the other hand, the goal of comparing results across projects and institutions requires standardization on normalization for entry into a databank.

4.3.1. Mitochondrial concentration, C_{mtE}, and mitochondrial markers: Mitochondrial organelles compose a dynamic cellular reticulum in various states of fusion and fission. Hence, the

definition of an 'amount' of mitochondria is often misconceived: mitochondria cannot be counted reliably as a number of occurring elementary components. Therefore, quantification of the amount of mitochondria depends on the measurement of chosen mitochondrial markers. '*Mitochondria are the structural and functional elementary units of cell respiration*' (Gnaiger 2014). The quantity of a mitochondrial marker can reflect the amount of mitochondrial elementary components, *mtE*, expressed in various mitochondrial elementary units [mtEU] specific for each measured mt-marker (**Table 4**). However, since mitochondrial quality may change in response to stimuli—particularly in mitochondrial dysfunction (Campos *et al.* 2017) and after exercise training (Pesta *et al.* 2011) and during aging (Daum *et al.* 2013)—some markers can vary while others are unchanged: (*1*) Mitochondrial volume and membrane area are structural markers, whereas mitochondrial protein mass is commonly used as a marker for isolated mitochondria. (*2*) Molecular and enzymatic mitochondrial markers (amounts or activities) can be selected as matrix markers, *e.g.*, citrate synthase activity, mtDNA; mtIM-markers, *e.g.*, cytochrome *c* oxidase activity, aa_3 content, cardiolipin, or mtOM-markers, *e.g.*, the voltage-dependent anion channel (VDAC), TOM20. (*3*) Extending the measurement of mitochondrial marker enzyme activity to mitochondrial pathway capacity, ET- or OXPHOS-capacity can be considered as an integrative functional mitochondrial marker.

Depending on the type of mitochondrial marker, the mitochondrial elementary component, *mtE*, is expressed in marker-specific units. Mitochondrial concentration in the instrumental chamber and mitochondrial density in the tissue of origin are quantified as (*1*) a quantity for normalization in functional analyses, C_{mtE}, and (*2*) a physiological output that is the result of mitochondrial biogenesis and degradation, D_{mtE}, respectively (**Table 4**). It is recommended, therefore, to distinguish *experimental mitochondrial concentration*, $C_{mtE} = mtE \cdot V^{-1}$ and *physiological mitochondrial density*, $D_{mtE} = mtE \cdot m_X^{-1}$. Then mitochondrial density is the amount of mitochondrial elementary components per mass of tissue, which is a biological variable (**Figure 6**). The experimental variable is mitochondrial density multiplied by sample mass concentration in the measuring chamber, $C_{mtE} = D_{mtE} \cdot C_{\underline{m}X}$, or mitochondrial content multiplied by sample number concentration, $C_{mtE} = mtE_X \cdot C_{\underline{N}X}$ (**Table 4**).

4.3.2. mt-Marker-specific flux, $J_{O2/mtE}$: Volume-specific metabolic O_2 flux depends on: (*1*) the sample concentration in the volume of the instrumental chamber, $C_{\underline{m}X}$, or $C_{\underline{N}X}$; (*2*) the mitochondrial density in the sample, $D_{mtE} = mtE \cdot m_X^{-1}$ or $mtE_X = mtE \cdot N_X^{-1}$; and (*3*) the specific mitochondrial activity or performance per mitochondrial elementary unit, $J_{O2/mtE} = J_{V,O2} \cdot C_{mtE}^{-1}$ [mol·s^{-1}·mtEU^{-1}] (**Table 4**). Obviously, the numerical results for $J_{O2/mtE}$ vary with the type of mitochondrial marker chosen for measurement of *mtE* and $C_{mtE} = mtE \cdot V^{-1}$ [mtEU·m^{-3}].

Different methods are involved in the quantification of mitochondrial markers and have different strengths and weaknesses. Some problems are common for all mitochondrial markers, *mtE*: (*1*) Accuracy of measurement is crucial, since even a highly accurate and reproducible measurement of chamber volume-specific O_2 flux results in an inaccurate and noisy expression if normalized by a biased and noisy measurement of a mitochondrial marker. This problem is acute in mitochondrial respiration because the denominators used (the mitochondrial markers) are often small moieties of which accurate and precise determination is difficult. In contrast, an *internal* marker is used when O_2 fluxes measured in substrate-uncoupler-inhibitor titration protocols are normalized for flux in a defined respiratory reference state within the assay, which yields flux control ratios, *FCR*s. *FCR*s are independent of externally measured markers and, therefore, are statistically robust, considering the limitations of ratios in general (Jasienski and Bazzaz 1999). *FCR*s indicate qualitative changes of mitochondrial respiratory control, with highest quantitative resolution, separating the effect of mitochondrial density on $J_{O2/\underline{m}X}$ and $I_{O2/\underline{N}X}$ from that of function per mitochondrial elementary marker, $J_{O2/mtE}$ (Pesta *et al.* 2011; Gnaiger 2014). (*2*) If mitochondrial quality does not change and only the amount of mitochondria varies as a determinant of mass-specific flux, any marker is equally qualified in principle; then in practice selection of the optimum marker depends only on the accuracy and precision of measurement of the mitochondrial marker. (*3*) If mitochondrial flux control ratios change, then there may not be any best mitochondrial marker. In general, measurement of multiple mitochondrial markers enables a comparison and evaluation of normalization for these mitochondrial markers. Particularly during postnatal development, the activity of marker enzymes—such as cytochrome *c* oxidase and citrate synthase—follows different time courses (Drahota *et al.* 2004). Evaluation of mitochondrial markers in healthy controls is insufficient for providing guidelines for application in the diagnosis of pathological states and specific treatments.

In line with the concept of the respiratory control ratio (Chance and Williams 1955a), the most readily used normalization is that of flux control ratios and flux control factors (Gnaiger 2014). Selection of the state of maximum flux in a protocol as the reference state has the advantages of: (*1*) internal normalization; (*2*) statistically validated linearization of the response in the range of 0 to 1; and (*3*) consideration of maximum flux for integrating a large number of elementary steps in the OXPHOS- or ET-pathways. This reduces the risk of selecting a functional marker that is specifically altered by the treatment or pathology, yet increases the chance that the highly integrative pathway is disproportionately affected, *e.g.*, the OXPHOS- rather than ET-pathway in case of an enzymatic defect in the phosphorylation-pathway. In this case, additional information can be obtained by reporting flux control ratios based on a reference state that indicates stable tissue-mass specific flux.

Stereological measurement of mitochondrial content via two-dimensional transmission electron microscopy is considered as the gold standard in determination of mitochondrial volume fractions in cells and tissues (Weibel, Hoppeler, 2005). Accurate determination of three-dimensional volume by two-dimensional microscopy, however, is both time consuming and statistically challenging (Larsen *et al.* 2012). The validity of using mitochondrial marker enzymes (citrate synthase activity, CI to CIV amount or activity) for normalization of flux is limited in part by the same factors that apply to flux control ratios. Strong correlations between various mitochondrial markers and citrate synthase activity (Reichmann *et al.* 1985; Boushel *et al.* 2007; Mogensen *et al.* 2007) are expected in a specific tissue of healthy persons and in disease states not specifically targeting citrate synthase. Citrate synthase activity is acutely modifiable by exercise (Tonkonogi *et al.* 1997; Leek *et al.* 2001). Evaluation of mitochondrial markers related to a selected age and sex cohort cannot be extrapolated to provide recommendations for normalization in respirometric diagnosis of disease, in different states of development and aging, different cell types, tissues, and species. mtDNA normalized to nDNA via qPCR is correlated to functional mitochondrial markers including OXPHOS- and ET-capacity in some cases (Puntschart *et al.* 1995; Wang *et al.* 1999; Menshikova *et al.* 2006; Boushel *et al.* 2007; Ehinger *et al.* 2015), but lack of such correlations have been reported (Menshikova *et al.* 2005; Schultz and Wiesner 2000; Pesta *et al.* 2011). Several studies indicate a strong correlation between cardiolipin content and increase in mitochondrial function with exercise (Menshikova *et al.* 2005; Menshikova *et al.* 2007; Larsen *et al.* 2012; Faber *et al.* 2014), but it has not been evaluated as a general mitochondrial biomarker in disease. With no single best mitochondrial marker, a good strategy is to quantify several different biomarkers to minimize the decorrelating effects caused by diseases, treatments, or other factors. Determination of multiple markers, particularly a matrix marker and a marker from the mtIM, allows tracking changes in mitochondrial quality defined by their ratio.

5. Normalization of rate per system

5.1. Flow: per chamber

The instrumental system (chamber) is part of the measurement instrument, separated from the environment as an isolated, closed, open, isothermal or non-isothermal system (**Table 4**). Reporting O_2 flows per respiratory chamber, I_{O_2} [nmol·s^{-1}], restricts the analysis to intra-experimental comparison of relative differences.

5.2. Flux: per chamber volume

5.2.1. System-specific flux, J_{V,O_2}: We distinguish between (*1*) the *system* with volume V and mass m defined by the system boundaries, and (*2*) the *sample* or *objects* with volume V_X and mass m_X that are enclosed in the instrumental chamber (**Figure 6**). Metabolic O_2 flow per object, $I_{O_2/\underline{N}X}$, is the total O_2 flow in the system divided by the number of objects, N_X, in the system. $I_{O_2/\underline{N}X}$ increases as the mass of the object is increased. Sample mass-specific O_2 flux, $J_{O_2/\underline{m}X}$ should be independent of the mass of the sample studied in the instrumental chamber, but system volume-specific O_2 flux, J_{V,O_2} (per volume of the instrumental chamber), increases in proportion to the mass of the sample in the chamber. Although J_{V,O_2} depends on mass-concentration of the sample in the chamber, it should be independent of the chamber (system) volume at constant sample mass-concentration. There are practical limitations to increasing the mass-concentration of the sample in the chamber, when one is concerned about crowding effects and instrumental time resolution.

5.2.2. Advancement per volume: When the reactor volume does not change during the reaction, which is typical for liquid phase reactions, the volume-specific *flux of a chemical reaction* r is the time derivative of the advancement of the reaction per unit volume, $J_{V,\mathrm{rB}} = \mathrm{d}_\mathrm{r}\xi_\mathrm{B}/\mathrm{d}t \cdot V^{-1}$ [(mol·s^{-1})·L^{-1}]. The *rate of concentration change* is $\mathrm{d}c_\mathrm{B}/\mathrm{d}t$ [(mol·L^{-1})·s^{-1}], where concentration is $c_\mathrm{B} = n_\mathrm{B} \cdot V^{-1}$. There is a difference between (*1*) $J_{V,\mathrm{rO_2}}$ [mol·s^{-1}·L^{-1}] and (*2*) rate of concentration change [mol·L^{-1}·s^{-1}]. These merge into a single expression only in closed systems. In open systems, internal transformations (catabolic flux, O_2 consumption) are distinguished from external flux (such as O_2 supply). External fluxes of all substances are zero in closed systems. In a closed chamber O_2 consumption (internal flux of catabolic reactions k; $I_{\mathrm{kO_2}}$ [pmol·s^{-1}]) causes a decline in the amount of O_2 in the system, $n_{\mathrm{O_2}}$ [nmol]. Normalization of these quantities for the volume of the system, V [L ≡ dm^3], yields volume-specific O_2 flux, $J_{V,\mathrm{kO_2}} = I_{\mathrm{kO_2}}/V$ [nmol·s^{-1}·L^{-1}], and O_2 concentration, [O_2] or $c_{\mathrm{O_2}} = n_{\mathrm{O_2}} \cdot V^{-1}$ [µmol·L^{-1} = µM = nmol·mL^{-1}]. Instrumental background O_2 flux is due to external flux into a non-ideal closed respirometer, so total volume-specific flux has to be corrected for instrumental background O_2 flux—O_2 diffusion into or out of the instrumental chamber. $J_{V,\mathrm{kO_2}}$ is relevant mainly for methodological reasons and should be compared with the accuracy of instrumental resolution of background-corrected flux, *e.g.*, ±1 nmol·s^{-1}·L^{-1} (Gnaiger 2001). 'Catabolic' indicates O_2 flux, $J_{\mathrm{kO_2}}$, corrected for: (*1*) instrumental background O_2 flux; (*2*) chemical background O_2 flux due to autoxidation of chemical components added to the incubation medium; and (*3*) *Rox* for O_2-consuming side reactions unrelated to the catabolic pathway k.

6. Conversion of units

Many different units have been used to report the O_2 consumption rate, OCR (**Table 6**). SI base units provide the common reference to introduce the theoretical principles (**Figure 6**), and are used with appropriately chosen SI prefixes to express numerical data in the most practical format, with an effort towards unification within specific areas of application (**Table 7**). Reporting data in SI units—including the mole [mol], coulomb [C], joule [J], and second [s]—should be encouraged, particularly by journals that propose the use of SI units.

Table 6. Conversion of various formats and units used in respirometry and ergometry. e$^-$ is the number of electrons or reducing equivalents. z_B is the charge number of entity B.

Format	1 Unit	·	Multiplication factor	SI-unit	Notes
$\underline{n}$	ng.atom O·s^{-1}	(2 e$^-$)	0.5	nmol O_2·s^{-1}	
$\underline{n}$	ng.atom O·min^{-1}	(2 e$^-$)	8.33	pmol O_2·s^{-1}	
$\underline{n}$	natom O·min^{-1}	(2 e$^-$)	8.33	pmol O_2·s^{-1}	
$\underline{n}$	nmol O_2·min^{-1}	(4 e$^-$)	16.67	pmol O_2·s^{-1}	
$\underline{n}$	nmol O_2·h^{-1}	(4 e$^-$)	0.2778	pmol O_2·s^{-1}	
$\underline{V}$ to $\underline{n}$	mL O_2·min^{-1} at STPD[a]		0.744	µmol O_2·s^{-1}	1
$\underline{e}$ to $\underline{n}$	W = J/s at -470 kJ/mol O_2		-2.128	µmol O_2·s^{-1}	
$\underline{e}$ to $\underline{n}$	mA = mC·s^{-1}	($z_{\mathrm{H^+}}$ = 1)	10.36	nmol H^+·s^{-1}	2
$\underline{e}$ to $\underline{n}$	mA = mC·s^{-1}	($z_{\mathrm{O_2}}$ = 4)	2.59	nmol O_2·s^{-1}	2
$\underline{n}$ to $\underline{e}$	nmol H^+·s^{-1}	($z_{\mathrm{H^+}}$ = 1)	0.09649	mA	3
$\underline{n}$ to $\underline{e}$	nmol O_2·s^{-1}	($z_{\mathrm{O_2}}$ = 4)	0.38594	mA	3

1 At standard temperature and pressure dry (STPD: 0 °C = 273.15 K and 1 atm = 101.325 kPa = 760 mmHg), the molar volume of an ideal gas, V_m, and $V_{\mathrm{m,O_2}}$ is 22.414 and 22.392 L·mol^{-1}, respectively. Rounded to three decimal places, both values yield the conversion factor of 0.744. For comparison at normal temperature and pressure dry (NTPD: 20 °C), $V_{\mathrm{m,O_2}}$ is 24.038 L·mol^{-1}. Note that the SI standard pressure is 100 kPa.

2 The multiplication factor is $10^6/(z_\mathrm{B} \cdot F)$.

3 The multiplication factor is $z_\mathrm{B} \cdot F/10^6$.

Table 7. Conversion of units with preservation of numerical values.

Name	Frequently used unit	Equivalent unit	Notes
volume-specific flux, J_{V,O_2}	pmol·s^{-1}·mL^{-1}	nmol·s^{-1}·L^{-1}	1
	mmol·s^{-1}·L^{-1}	mol·s^{-1}·m^{-3}	
cell-specific flow, $I_{O_2/\underline{N}ce}$	pmol·s^{-1}·10^{-6} cells	amol·s^{-1}·cell^{-1}	2
	pmol·s^{-1}·10^{-9} cells	zmol·s^{-1}·cell^{-1}	3
cell number concentration, $C_{\underline{N}ce}$	10^6 cells·mL^{-1}	10^9 cells·L^{-1}	
mitochondrial protein concentration, C_{mtE}	0.1 mg·mL^{-1}	0.1 g·L^{-1}	
mass-specific flux, $J_{O_2/\underline{m}}$	pmol·s^{-1}·mg^{-1}	nmol·s^{-1}·g^{-1}	4
catabolic power, P_k	µW·10^{-6} cells	pW·cell^{-1}	1
volume	1,000 L	m^3 (1,000 kg)	
	L	dm^3 (kg)	
	mL	cm^3 (g)	
	µL	mm^3 (mg)	
	fL	µm^3 (pg)	5
amount of substance concentration	M = mol·L^{-1}	mol·dm^{-3}	

1 pmol: picomole = 10^{-12} mol
2 amol: attomole = 10^{-18} mol
3 zmol: zeptomole = 10^{-21} mol
4 nmol: nanomole = 10^{-9} mol
5 fL: femtolitre = 10^{-15} L

Although volume is expressed as m^3 using the SI base unit, the litre [dm^3] is a conventional unit of volume for concentration and is used for most solution chemical kinetics. If one multiplies $I_{O_2/\underline{N}ce}$ by $C_{\underline{N}ce}$, then the result will not only be the amount of O_2 [mol] consumed per time [s^{-1}] in one litre [L^{-1}], but also the change in O_2 concentration per second (for any volume of an ideally closed system). This is ideal for kinetic modeling as it blends with chemical rate equations where concentrations are typically expressed in mol·L^{-1} (Wagner *et al.* 2011). In studies of multinuclear cells—such as differentiated skeletal muscle cells—it is easy to determine the number of nuclei but not the total number of cells. A generalized concept, therefore, is obtained by substituting cells by nuclei as the sample entity. This does not hold, however, for non-nucleated platelets.

For studies of cells, we recommend that respiration be expressed, as far as possible, as: (*1*) O_2 flux normalized for a mitochondrial marker, for separation of the effects of mitochondrial quality and content on cell respiration (this includes *FCR*s as a normalization for a functional mitochondrial marker); (*2*) O_2 flux in units of cell volume or mass, for comparison of respiration of cells with different cell size (Renner *et al.* 2003) and with studies on tissue preparations, and (*3*) O_2 flow in units of attomole (10^{-18} mol) of O_2 consumed per second by each cell [amol·s^{-1}·cell^{-1}], numerically equivalent to [pmol·s^{-1}·10^{-6} cells]. This convention allows information to be easily used when designing experiments in which O_2 flow must be considered. For example, to estimate the volume-specific O_2 flux in an instrumental chamber that would be expected at a particular cell number concentration, one simply needs to multiply the flow per cell by the number of cells per volume of interest. This provides the amount of O_2 [mol] consumed per time [s^{-1}] per unit volume [L^{-1}]. At an O_2 flow of 100 amol·s^{-1}·cell^{-1} and a cell concentration of 10^9 cells·L^{-1} (10^6 cells·mL^{-1}), the volume-specific O_2 flux is 100 nmol·s^{-1}·L^{-1} (100 pmol·s^{-1}·mL^{-1}).

ET-capacity in human cell types including HEK 293, primary HUVEC, and fibroblasts ranges from 50 to 180 amol·s^{-1}·cell^{-1}, measured in living cells in the noncoupled state (see Gnaiger 2014). At 100 amol·s^{-1}·cell^{-1} corrected for *Rox*, the current across the mt-membranes, I_{H^+e}, approximates 193 pA·cell^{-1} or 0.2 nA per cell. See Rich (2003) for an extension of quantitative bioenergetics from the molecular to the human scale, with a transmembrane proton flux equivalent to 520 A in an adult at a catabolic power of -110 W. Modelling approaches illustrate the link between protonmotive force and currents (Willis *et al.* 2016).

We consider isolated mitochondria as powerhouses and proton pumps as molecular machines to relate experimental results to energy metabolism of living cells. The cellular P»/O_2 based on oxidation

of glycogen is increased by the glycolytic (fermentative) substrate-level phosphorylation of 3 P»/Glyc or 0.5 mol P» for each mol O_2 consumed in the complete oxidation of a mol glycosyl unit (Glyc). Adding 0.5 to the mitochondrial P»/O_2 ratio of 5.4 yields a bioenergetic cell physiological P»/O_2 ratio close to 6. Two NADH equivalents are formed during glycolysis and transported from the cytosol into the mitochondrial matrix, either by the malate-aspartate shuttle or by the glycerophosphate shuttle (**Figure 2A**) resulting in different theoretical yields of ATP generated by mitochondria, the energetic cost of which potentially must be taken into account. Considering also substrate-level phosphorylation in the TCA cycle, this high P»/O_2 ratio not only reflects proton translocation and OXPHOS studied in isolation, but integrates mitochondrial physiology with energy transformation in the living cell (Gnaiger 1993a).

7. Conclusions

Catabolic cell respiration is the process of exergonic and exothermic energy transformation in which scalar redox reactions are coupled to vectorial ion translocation across a semipermeable membrane, which separates the small volume of a bacterial cell or mitochondrion from the larger volume of its surroundings. The electrochemical exergy can be partially conserved in the phosphorylation of ADP to ATP or in ion pumping, or dissipated in an electrochemical short-circuit. Respiration is thus clearly distinguished from fermentation as the counterparts of cellular core energy metabolism. An O_2 flux balance scheme illustrates the relationships and general definitions (**Figures 1 and 2**).

Box 3: Recommendations for studies with mitochondrial preparations

- Normalization of respiratory rates should be provided as far as possible:
  - A. Sample normalization
    1. *Object-specific biophysical normalization*: on a per organism or per cell basis as O_2 flow; this may not be possible when dealing with coenocytic organisms, *e.g.*, filamentous fungi, or tissues without cross-walls separating individual cells, *e.g.*, muscle fibers.
    2. *Size-specific cellular normalization*: per g protein; per organism-, cell- or tissue-mass as mass-specific O_2 flux; per cell volume as cell volume-specific flux.
    3. *Mitochondrial normalization*: per mitochondrial marker as mt-specific flux.
  - B. Chamber normalization
    1. Chamber volume-specific flux, J_V [pmol·s^{-1}·mL^{-1}], is reported for quality control in relation to instrumental sensitivity and limit of detection of volume-specific flux.
    2. Sample concentration in the instrumental chamber is reported as number concentration, mass concentration, or mitochondrial concentration; this is a component of the measuring conditions.

  With information on cell size and the use of multiple normalizations, maximum potential information is available (Renner *et al.* 2003; Wagner *et al.* 2011; Gnaiger 2014). Reporting flow in a respiratory chamber [nmol·s^{-1}] is discouraged, since it restricts the analysis to intra-experimental comparison of relative (qualitative) differences.
- Catabolic mitochondrial respiration is distinguished from residual O_2 consumption. Fluxes in mitochondrial coupling states should be, as far as possible, corrected for residual O_2 consumption.
- Different mechanisms of uncoupling should be distinguished by defined terms. The tightness of coupling relates to these uncoupling mechanisms, whereas the coupling stoichiometry varies as a function the substrate type involved in ET-pathways with either three or two redox proton pumps operating in series. Separation of tightness of coupling from the pathway-dependent coupling stoichiometry is possible only when the substrate type undergoing oxidation remains the same for respiration in LEAK-, OXPHOS-, and ET-states. In studies of the tightness of coupling, therefore, simple substrate-inhibitor combinations should be applied to exlcude a shift in substrate competition that may occur when providing physiological substrate cocktails.
- In studies of isolated mitochondria, the mitochondrial recovery and yield should be reported. Experimental criteria such as transmission electron microscopy for evaluation of purity versus integrity should be considered. Mitochondrial markers—such as citrate synthase activity as an enzymatic matrix marker—provide a link to the tissue of origin on the basis of calculating the mitochondrial recovery, *i.e.*, the fraction of mitochondrial marker obtained from a unit mass of tissue.

Total mitochondrial protein is frequently applied as a mitochondrial marker, which is restricted to isolated mitochondria.

- In studies of permeabilized cells, the viability of the cell culture or cell suspension of origin should be reported. Normalization should be evaluated for total cell count or viable cell count.
- Terms and symbols are summarized in **Table 8**. Their use will facilitate transdisciplinary communication and support further development of a consistent theory of bioenergetics and mitochondrial physiology. Technical terms related to and defined with normal words can be used as index terms in databases, support the creation of ontologies towards semantic information processing (MitoPedia), and help in communicating analytical findings as impactful data-driven stories. '*Making data available without making it understandable may be worse than not making it available at all*' (National Academies of Sciences, Engineering, and Medicine 2018). Success will depend on taking further steps: (*1*) exhaustive text-mining considering Omics data and functional data; (*2*) network analysis of Omics data with bioinformatics tools; (*3*) cross-validation with distinct bioinformatics approaches; (*4*) correlation with physiological data; (*5*) guidelines for biological validation of network data. This is a call to carefully contribute to FAIR principles (Findable, Accessible, Interoperable, Reusable) for the sharing of scientific data.

Table 8. Terms, symbols, and units.

Term	Symbol	Unit	Links and comments
alternative quinol oxidase	AOX		Figure 2B
adenosine monophosphate	AMP		2 ADP ↔ ATP+AMP
adenosine diphosphate	ADP		Table 1; Figures 1, 2 and 5
adenosine triphosphate	ATP		Figures 2 and 5
adenylates	AMP, ADP, ATP		Section 2.5.1
amount of substance B	n_B	[mol]	
ATP yield per O_2	$Y_{P»/O_2}$		P»/O_2 ratio measured in any respiratory state
catabolic reaction	k		Figures 1 and 3
catabolic respiration	J_{kO_2}	*varies*	Figures 1 and 3
cell concentration (mass)	$C_{\underline{m}ce}$	[kg·m^{-3}]	Table 4
cell concentration (number)	$C_{\underline{N}ce}$	[x·m^{-3}]	Table 4
cell respiration	J_{rO_2}	*varies*	Figure 1
cell viability index	*VI*		$VI = N_{vce} \cdot N_{ce}^{-1} = 1 - N_{dce} \cdot N_{ce}^{-1}$
charge number of entity B	z_B		Table 6; $z_{O_2} = 4$
Complexes I to IV	CI to CIV		respiratory ET Complexes; Figure 2B
concentration of substance B	$c_B = n_B \cdot V^{-1}$; [B]	[mol·m^{-3}]	Box 2
coupling control state	CCS		Section 2.4.1
electric format	$\underline{e}$	[C]	Table 6
electron transfer system	ETS		state; Figures 2B and 4
ET state	ET		Table 1; Figures 2B and 4; State 3u
ET-capacity	*E*	*varies*	Table 1; Figure 4
flow, for substance B	I_B	[mol·s^{-1}]	system-related extensive quantity; Figure 6
flux, for substance B	J_B	*varies*	size-specific quantitiy; Figure 6
inorganic phosphate	P_i		Figure 2C
inorganic phosphate carrier	PiC		Figure 2C
LEAK state	LEAK		state; Table 1; Figure 4; compare State 4
LEAK-respiration	*L*	*varies*	Table 1; Figure 4
mass format	$\underline{m}$	[kg]	Table 4; Figure 6
mass of sample *X*	m_X	[kg]	Table 4

mass, dry mass	m_d	[kg]	mass of sample *X*; Figure 6 (frequently called dry weight)
mass, wet mass	m_w	[kg]	mass of sample *X*; Figure 6 (frequently called wet weight)
mass of object *X*	$m_{\underline{N}X} = m_X \cdot N_X^{-1}$	[kg·x^{-1}]	mass of entity *X*; Table 4
MITOCARTA			https://www.broadinstitute.org/scientific-community/science/programs/metabolic-disease-program/publications/mitocarta/mitocarta-in-0
MitoPedia			http://www.bioblast.at/index.php/MitoPedia
mitochondria or mitochondrial	mt		Box 1
mitochondrial DNA	mtDNA		Box 1
mitochondrial concentration	$C_{mtE} = mtE \cdot V^{-1}$	[mtEU·m^{-3}]	Table 4
mitochondrial content	mtE_X	[mtEU·x^{-1}]	$mtE_X = mtE \cdot N_X^{-1}$; Table 4
mitochondrial elementary component	*mtE*	[mtEU]	quantity of mt-marker; Table 4
mitochondrial elementary unit	mtEU	*varies*	specific units for mt-marker; Table 4
mitochondrial inner membrane	mtIM		MIM is widely used; the first M is replaced by mt; Figure 2; Box 1
mitochondrial outer membrane	mtOM		MOM is widely used; the first M is replaced by mt; Figure 2; Box 1
mitochondrial recovery	Y_{mtE}		fraction of *mtE* recovered in sample from the tissue of origin
mitochondrial yield	$Y_{mtE/\underline{m}}$		mt-yield per tissues mass; $Y_{mtE/\underline{m}} = Y_{mtE} \cdot D_{mtE}$
molar format	$\underline{n}$	[mol]	Table 6
negative	neg		Figure 4
number concentration of *X*	$C_{\underline{N}X}$	[x·m^{-3}]	Table 4
number format	$\underline{N}$	[x]	Table 4; Figure 6
number of cells	N_{ce}	[x]	total cell count of living cells, $N_{ce} = N_{vce} + N_{dce}$; Table 5
number of dead cells	N_{dce}	[x]	non-viable cells, loss of plasma membrane barrier function; Table 5
number of entities *X*	N_X	[x]	Table 4; Figure 6
number of entity B	N_B	[x]	Table 4
number of viable cells	N_{vce}	[x]	viable cells, intact plasma membrane barrier function; Table 5
oxidative phosphorylation	OXPHOS		state; Table 1; Figure 4
OXPHOS state	OXPHOS		Table 1; State 3 if [ADP] and [P_i] are kinetically-saturating
OXPHOS-capacity	*P*	*varies*	Table 1; Figure 4
oxygen concentration	$c_{O_2} = n_{O_2} \cdot V^{-1}$	[mol·m^{-3}]	[O_2]; Section 3.2
oxygen flux, in reaction r	J_{rO_2}	*varies*	Figure 1
pathway control state	PCS		Section 2.2
permeability transition	mtPT		Figure 3; Section 2.4.3; MPT is widely used; M is replaced by mt
permeabilized cell number	N_{pce}	[x]	experimental permeabilization of plasma membrane; Table 5
phosphorylation of ADP to ATP	P»		Section 2.2
P»/O_2 ratio	P»/O_2		mechanistic $Y_{P»/O_2}$, calculated from pump stoichiometries; Figure 2B
positive	pos		Figure 4
proton in the negative compartment	H^+_{neg}		Figure 4
proton in the positive compartment	H^+_{pos}		Figure 4
protonmotive force	pmf	[V]	Figures 1, 2A and 4; Table 1

rate of electron transfer in ET state	*E*	*varies*	ET-capacity; Table 1
rate of LEAK-respiration	*L*	*varies*	Table 1: *L*(n), *L*(T), *L*(Omy)
rate of oxidative phosphorylation	*P*	*varies*	OXPHOS-capacity; Table 1
rate of residual oxygen consumption	*Rox*		Table 1; Figure 1
residual oxygen consumption	ROX; *Rox*		state ROX; rate *Rox*; Table 1
respiratory supercomplex	SC $I_nIII_nIV_n$		supramolecular assemblies composed of variable copy numbers (*n*) of CI, CIII and CIV; Box 1
specific mitochondrial density	$D_{mtE} = mtE \cdot m_X^{-1}$	[mtEU·kg^{-1}]	Table 4
substrate concentration at half-maximal rate	c_{50}	[mol·m^{-3}]	Section 2.1.2
substrate-uncoupler-inhibitor-titration protocol	SUIT		Section 2.2
volume	*V*	[m^{-3}]	Table 7
volume format	$\underline{V}$	[m^{-3}]	Table 6

Experimentally, respiration is separated in mitochondrial preparations from the interactions with the fermentative pathways of the living cell. OXPHOS analysis is based on the study of mitochondrial preparations complementary to bioenergetic investigations of (*1*) submitochondrial particles and molecular structures, (*2*) living cells, and (*3*) organisms—from model organisms to the human species including healthy and diseased persons (patients). Different mechanisms of respiratory uncoupling have to be distinguished (**Figure 3**). Metabolic fluxes measured in defined coupling and pathway control states (**Figures 5 and 6**) provide insights into the meaning of cellular and organismic respiration.

The optimal choice for expressing mitochondrial and cell respiration as O_2 flow per biological sample, and normalization for specific tissue-markers (volume, mass, protein) and mitochondrial markers (volume, protein, content, mtDNA, activity of marker enzymes, respiratory reference state) is guided by the scientific question under study. Interpretation of the data depends critically on appropriate normalization (**Figure 6**).

MitoEAGLE can serve as a gateway to better diagnose mitochondrial respiratory adaptations and defects linked to genetic variation, age-related health risks, sex-specific mitochondrial performance, lifestyle with its effects on degenerative diseases, and thermal and chemical environment. The present recommendations on coupling control states and rates are focused on studies using mitochondrial preparations (**Box 3**). These will be extended in a series of reports on pathway control of mitochondrial respiration, respiratory states and rates in living cells, respiratory flux control ratios, and harmonization of experimental procedures.

Acknowledgements

We thank Beno M for management assistance, and Rich PR for valuable discussions. This publication is based upon work from COST Action CA15203 MitoEAGLE, supported by COST (European Cooperation in Science and Technology), in cooperation with COST Actions CA16225 EU-CARDIOPROTECTION and CA17129 CardioRNA, and K-Regio project MitoFit funded by the Tyrolian Government.

Author contributions

This manuscript developed as an open invitation to scientists and students to join as coauthors in the bottom-up spirit of COST, based on a first draft written by the corresponding author, who integrated coauthor contributions in a sequence of Open Access versions. Coauthors contributed to the scope and quality of the manuscript, may have focused on a particular section, and are listed in alphabetical order. Coauthors confirm that they have read the final manuscript and agree to implement the recommendations into future manuscripts, presentations and teaching materials.

Competing financial interests: E.G. is founder and CEO of Oroboros Instruments, Innsbruck, Austria.

References

Altmann R (1894) Die Elementarorganismen und ihre Beziehungen zu den Zellen. Zweite vermehrte Auflage. Verlag Von Veit & Comp, Leipzig:160 pp.

Baggeto LG, Testa-Perussini R (1990) Role of acetoin on the regulation of intermediate metabolism of Ehrlich ascites tumor mitochondria: its contribution to membrane cholesterol enrichment modifying passive proton permeability. Arch Biochem Biophys 283:341-8.

Beard DA (2005) A biophysical model of the mitochondrial respiratory system and oxidative phosphorylation. PLoS Comput Biol 1(4):e36.

Benda C (1898) Weitere Mitteilungen über die Mitochondria. Verh Dtsch Physiol Ges:376-83.

Birkedal R, Laasmaa M, Vendelin M (2014) The location of energetic compartments affects energetic communication in cardiomyocytes. Front Physiol 5:376.

Blier PU, Dufresne F, Burton RS (2001) Natural selection and the evolution of mtDNA-encoded peptides: evidence for intergenomic co-adaptation. Trends Genet 17:400-6.

Blier PU, Guderley HE (1993) Mitochondrial activity in rainbow trout red muscle: the effect of temperature on the ADP-dependence of ATP synthesis. J Exp Biol 176:145-58.

Breton S, Beaupré HD, Stewart DT, Hoeh WR, Blier PU (2007) The unusual system of doubly uniparental inheritance of mtDNA: isn't one enough? Trends Genet 23:465-74.

Brown GC (1992) Control of respiration and ATP synthesis in mammalian mitochondria and cells. Biochem J 284:1-13.

Burger G, Gray MW, Forget L, Lang BF (2013) Strikingly bacteria-like and gene-rich mitochondrial genomes throughout jakobid protists. Genome Biol Evol 5:418-38.

Calvo SE, Klauser CR, Mootha VK (2016) MitoCarta2.0: an updated inventory of mammalian mitochondrial proteins. Nucleic Acids Research 44:D1251-7.

Calvo SE, Julien O, Clauser KR, Shen H, Kamer KJ, Wells JA, Mootha VK (2017) Comparative analysis of mitochondrial N-termini from mouse, human, and yeast. Mol Cell Proteomics 16:512-23.

Campos JC, Queliconi BB, Bozi LHM, Bechara LRG, Dourado PMM, Andres AM, Jannig PR, Gomes KMS, Zambelli VO, Rocha-Resende C, Guatimosim S, Brum PC, Mochly-Rosen D, Gottlieb RA, Kowaltowski AJ, Ferreira JCB (2017) Exercise reestablishes autophagic flux and mitochondrial quality control in heart failure. Autophagy 13:1304-317.

Canton M, Luvisetto S, Schmehl I, Azzone GF (1995) The nature of mitochondrial respiration and discrimination between membrane and pump properties. Biochem J 310:477-81.

Carrico C, Meyer JG, He W, Gibson BW, Verdin E (2018) The mitochondrial acylome emerges: proteomics, regulation by Sirtuins, and metabolic and disease implications. Cell Metab 27:497-512.

Chan DC (2006) Mitochondria: dynamic organelles in disease, aging, and development. Cell 125:1241-52.

Chance B, Williams GR (1955a) Respiratory enzymes in oxidative phosphorylation. I. Kinetics of oxygen utilization. J Biol Chem 217:383-93.

Chance B, Williams GR (1955b) Respiratory enzymes in oxidative phosphorylation: III. The steady state. J Biol Chem 217:409-27.

Chance B, Williams GR (1955c) Respiratory enzymes in oxidative phosphorylation. IV. The respiratory chain. J Biol Chem 217:429-38.

Chance B, Williams GR (1956) The respiratory chain and oxidative phosphorylation. Adv Enzymol Relat Subj Biochem 17:65-134.

Chowdhury SK, Djordjevic J, Albensi B, Fernyhough P (2015) Simultaneous evaluation of substrate-dependent oxygen consumption rates and mitochondrial membrane potential by TMRM and safranin in cortical mitochondria. Biosci Rep 36:e00286.

Cobb LJ, Lee C, Xiao J, Yen K, Wong RG, Nakamura HK, Mehta HH, Gao Q, Ashur C, Huffman DM, Wan J, Muzumdar R, Barzilai N, Cohen P (2016) Naturally occurring mitochondrial-derived peptides are age-dependent regulators of apoptosis, insulin sensitivity, and inflammatory markers. Aging (Albany NY) 8:796-809.

Cohen ER, Cvitas T, Frey JG, Holmström B, Kuchitsu K, Marquardt R, Mills I, Pavese F, Quack M, Stohner J, Strauss HL, Takami M, Thor HL (2008) Quantities, units and smbols in physical chemistry, IUPAC Green Book, 3rd Edition, 2nd Printing, IUPAC & RSC Publishing, Cambridge.

Cooper H, Hedges LV, Valentine JC, eds (2009) The handbook of research synthesis and meta-analysis. Russell Sage Foundation.

Coopersmith J (2010) Energy, the subtle concept. The discovery of Feynman's blocks from Leibnitz to Einstein. Oxford University Press:400 pp.

Cummins J (1998) Mitochondrial DNA in mammalian reproduction. Rev Reprod 3:172-82.

Dai Q, Shah AA, Garde RV, Yonish BA, Zhang L, Medvitz NA, Miller SE, Hansen EL, Dunn CN, Price TM (2013) A truncated progesterone receptor (PR-M) localizes to the mitochondrion and controls cellular respiration. Mol Endocrinol 27:741-53.

Daum B, Walter A, Horst A, Osiewacz HD, Kühlbrandt W (2013) Age-dependent dissociation of ATP synthase dimers and loss of inner-membrane cristae in mitochondria. Proc Natl Acad Sci U S A 110:15301-6.

Diebold LP, Gil HJ, Gao P, Martinez CA, Weinberg SE, Chandel NS (2019) Mitochondrial Complex III is necessary for endothelial cell proliferation during angiogenesis. Nat Metab 1:158–71.

Divakaruni AS, Brand MD (2011) The regulation and physiology of mitochondrial proton leak. Physiology (Bethesda) 26:192-205.

Doerrier C, Garcia-Souza LF, Krumschnabel G, Wohlfarter Y, Mészáros AT, Gnaiger E (2018) High-Resolution FluoRespirometry and OXPHOS protocols for human cells, permeabilized fibres from small biopsies of muscle, and isolated mitochondria. Methods Mol Biol 1782 (Palmeira CM, Moreno AJ, eds): Mitochondrial Bioenergetics, 978-1-4939-7830-4.

Doskey CM, van 't Erve TJ, Wagner BA, Buettner GR (2015) Moles of a substance per cell is a highly informative dosing metric in cell culture. PLoS One 10:e0132572.

Drahota Z, Milerová M, Stieglerová A, Houstek J, Ostádal B (2004) Developmental changes of cytochrome *c* oxidase and citrate synthase in rat heart homogenate. Physiol Res 53:119-22.

Duarte FV, Palmeira CM, Rolo AP (2014) The role of microRNAs in mitochondria: small players acting wide. Genes (Basel) 5:865-86.

Ehinger JK, Morota S, Hansson MJ, Paul G, Elmér E (2015) Mitochondrial dysfunction in blood cells from amyotrophic lateral sclerosis patients. J Neurol 262:1493-503.

Ehinger JK, Piel S, Ford R, Karlsson M, Sjövall F, Frostner EÅ, Morota S, Taylor RW, Turnbull DM, Cornell C, Moss SJ, Metzsch C, Hansson MJ, Fliri H, Elmér E (2016) Cell-permeable succinate prodrugs bypass mitochondrial complex I deficiency. Nat Commun 7:12317.

Ernster L, Schatz G (1981) Mitochondria: a historical review. J Cell Biol 91:227s-55s.

Estabrook RW (1967) Mitochondrial respiratory control and the polarographic measurement of ADP:O ratios. Methods Enzymol 10:41-7.

Faber C, Zhu ZJ, Castellino S, Wagner DS, Brown RH, Peterson RA, Gates L, Barton J, Bickett M, Hagerty L, Kimbrough C, Sola M, Bailey D, Jordan H, Elangbam CS (2014) Cardiolipin profiles as a potential biomarker of mitochondrial health in diet-induced obese mice subjected to exercise, diet-restriction and ephedrine treatment. J Appl Toxicol 34:1122-9.

Feagin JE, Harrell MI, Lee JC, Coe KJ, Sands BH, Cannone JJ, Tami G, Schnare MN, Gutell RR (2012) The fragmented mitochondrial ribosomal RNAs of *Plasmodium falciparum*. PLoS One 7:e38320.

Fell D (1997) Understanding the control of metabolism. Portland Press.

Forstner H, Gnaiger E (1983) Calculation of equilibrium oxygen concentration. In: Polarographic Oxygen Sensors. Aquatic and Physiological Applications. Gnaiger E, Forstner H (eds), Springer, Berlin, Heidelberg, New York:321-33.

Garlid KD, Beavis AD, Ratkje SK (1989) On the nature of ion leaks in energy-transducing membranes. Biochim Biophys Acta 976:109-20.

Garlid KD, Semrad C, Zinchenko V. Does redox slip contribute significantly to mitochondrial respiration? In: Schuster S, Rigoulet M, Ouhabi R, Mazat J-P, eds (1993) Modern trends in biothermokinetics. Plenum Press, New York, London:287-93.

Gebert N, Joshi AS, Kutik S, Becker T, McKenzie M, Guan XL, Mooga VP, Stroud DA, Kulkarni G, Wenk MR, Rehling P, Meisinger C, Ryan MT, Wiedemann N, Greenberg ML, Pfanner N (2009) Mitochondrial cardiolipin involved in outer-membrane protein biogenesis: implications for Barth syndrome. Curr Biol 19:2133-9.

Gerö D, Szabo C (2016) Glucocorticoids suppress mitochondrial oxidant production via upregulation of uncoupling protein 2 in hyperglycemic endothelial cells. PLoS One 11:e0154813.

Gibney E (2018) Largest overhaul of scientific units since 1875 wins approval. Nature 563:451–2. https://www.nature.com/articles/d41586-018-07424-8

Gnaiger E. Efficiency and power strategies under hypoxia. Is low efficiency at high glycolytic ATP production a paradox? In: Surviving Hypoxia: Mechanisms of Control and Adaptation. Hochachka PW, Lutz PL, Sick T, Rosenthal M, Van den Thillart G, eds (1993a) CRC Press, Boca Raton, Ann Arbor, London, Tokyo:77-109.

Gnaiger E (1993b) Nonequilibrium thermodynamics of energy transformations. Pure Appl Chem 65:1983-2002.

Gnaiger E (2001) Bioenergetics at low oxygen: dependence of respiration and phosphorylation on oxygen and adenosine diphosphate supply. Respir Physiol 128:277-97.

Gnaiger E (2009) Capacity of oxidative phosphorylation in human skeletal muscle. New perspectives of mitochondrial physiology. Int J Biochem Cell Biol 41:1837-45.

Gnaiger E (2014) Mitochondrial pathways and respiratory control. An introduction to OXPHOS analysis. 4th ed. Mitochondr Physiol Network 19.12. Oroboros MiPNet Publications, Innsbruck:80 pp.

Gnaiger E, Méndez G, Hand SC (2000) High phosphorylation efficiency and depression of uncoupled respiration in mitochondria under hypoxia. Proc Natl Acad Sci USA 97:11080-5.

Greggio C, Jha P, Kulkarni SS, Lagarrigue S, Broskey NT, Boutant M, Wang X, Conde Alonso S, Ofori E, Auwerx J, Cantó C, Amati F (2017) Enhanced respiratory chain supercomplex formation in response to exercise in human skeletal muscle. Cell Metab 25:301-11.

Hinkle PC (2005) P/O ratios of mitochondrial oxidative phosphorylation. Biochim Biophys Acta 1706:1-11.

Hofstadter DR (1979) Gödel, Escher, Bach: An eternal golden braid. A metaphorical fugue on minds and machines in the spirit of Lewis Carroll. Harvester Press:499 pp.

Illaste A, Laasmaa M, Peterson P, Vendelin M (2012) Analysis of molecular movement reveals latticelike obstructions to diffusion in heart muscle cells. Biophys J 102:739-48.

Jasienski M, Bazzaz FA (1999) The fallacy of ratios and the testability of models in biology. Oikos 84:321-26.

Jepihhina N, Beraud N, Sepp M, Birkedal R, Vendelin M (2011) Permeabilized rat cardiomyocyte response demonstrates intracellular origin of diffusion obstacles. Biophys J 101:2112-21.

Jezek P, Holendova B, Garlid KD, Jaburek M (2018) Mitochondrial uncoupling proteins: subtle regulators of cellular redox signaling. Antioxid Redox Signal 29:667-714.

Karnkowska A, Vacek V, Zubáčová Z, Treitli SC, Petrželková R, Eme L, Novák L, Žárský V, Barlow LD, Herman EK, Soukal P, Hroudová M, Doležal P, Stairs CW, Roger AJ, Eliáš M, Dacks JB, Vlček Č, Hampl V (2016) A eukaryote without a mitochondrial organelle. Curr Biol 26:1274-84.

Kenwood BM, Weaver JL, Bajwa A, Poon IK, Byrne FL, Murrow BA, Calderone JA, Huang L, Divakaruni AS, Tomsig JL, Okabe K, Lo RH, Cameron Coleman G, Columbus L, Yan Z, Saucerman JJ, Smith JS, Holmes JW, Lynch KR, Ravichandran KS, Uchiyama S, Santos WL, Rogers GW, Okusa MD, Bayliss DA, Hoehn KL (2013) Identification of a novel mitochondrial uncoupler that does not depolarize the plasma membrane. Mol Metab 3:114-23.

Klepinin A, Ounpuu L, Guzun R, Chekulayev V, Timohhina N, Tepp K, Shevchuk I, Schlattner U, Kaambre T (2016) Simple oxygraphic analysis for the presence of adenylate kinase 1 and 2 in normal and tumor cells. J Bioenerg Biomembr 48:531-48.

Koit A, Shevchuk I, Ounpuu L, Klepinin A, Chekulayev V, Timohhina N, Tepp K, Puurand M,Truu L, Heck K, Valvere V, Guzun R, Kaambre T (2017) Mitochondrial respiration in human colorectal and breast cancer clinical material is regulated differently. Oxid Med Cell Longev 1372640.

Komlódi T, Tretter L (2017) Methylene blue stimulates substrate-level phosphorylation catalysed by succinyl-CoA ligase in the citric acid cycle. Neuropharmacology 123:287-98.

Korn E (1969) Cell membranes: structure and synthesis. Annu Rev Biochem 38:263–88.

Lai N, M Kummitha C, Rosca MG, Fujioka H, Tandler B, Hoppel CL (2018) Isolation of mitochondrial subpopulations from skeletal muscle: optimizing recovery and preserving integrity. Acta Physiol (Oxf):e13182. doi: 10.1111/apha.13182.

Lane N (2005) Power, sex, suicide: mitochondria and the meaning of life. Oxford University Press:354 pp.

Larsen S, Nielsen J, Neigaard Nielsen C, Nielsen LB, Wibrand F, Stride N, Schroder HD, Boushel RC, Helge JW, Dela F, Hey-Mogensen M (2012) Biomarkers of mitochondrial content in skeletal muscle of healthy young human subjects. J Physiol 590:3349-60.

Lee C, Zeng J, Drew BG, Sallam T, Martin-Montalvo A, Wan J, Kim SJ, Mehta H, Hevener AL, de Cabo R, Cohen P (2015) The mitochondrial-derived peptide MOTS-c promotes metabolic homeostasis and reduces obesity and insulin resistance. Cell Metab 21:443-54.

Lee SR, Kim HK, Song IS, Youm J, Dizon LA, Jeong SH, Ko TH, Heo HJ, Ko KS, Rhee BD, Kim N, Han J (2013) Glucocorticoids and their receptors: insights into specific roles in mitochondria. Prog Biophys Mol Biol 112:44-54.

Leek BT, Mudaliar SR, Henry R, Mathieu-Costello O, Richardson RS (2001) Effect of acute exercise on citrate synthase activity in untrained and trained human skeletal muscle. Am J Physiol Regul Integr Comp Physiol 280:R441-7.

Lemasters JJ, Nieminen AL, Qian T, Trost LC, Elmore SP, Nishimura Y, Crowe RA, Cascio WE, Bradham CA, Brenner DA, Herman B (1998) The mitochondrial permeability transition in cell death: a common mechanism in necrosis, apoptosis and autophagy. Biochim Biophys Acta 1366:177-96.

Lemieux H, Blier PU, Gnaiger E (2017) Remodeling pathway control of mitochondrial respiratory capacity by temperature in mouse heart: electron flow through the Q-junction in permeabilized fibers. Sci Rep 7:2840.

Lemieux H, Semsroth S, Antretter H, Höfer D, Gnaiger E (2011) Mitochondrial respiratory control and early defects of oxidative phosphorylation in the failing human heart. Int J Biochem Cell Biol 43:1729–38.

Lenaz G, Tioli G, Falasca AI, Genova ML (2017) Respiratory supercomplexes in mitochondria. In: Mechanisms of primary energy trasduction in biology. M Wikstrom (ed) Royal Society of Chemistry Publishing, London, UK:296-337.

Liu S, Roellig DM, Guo Y, Li N, Frace MA, Tang K, Zhang L, Feng Y, Xiao L (2016) Evolution of mitosome metabolism and invasion-related proteins in *Cryptosporidium*. BMC Genomics 17:1006.

Lisowski P, Kannan P, Mlody B, Prigione A (2018) Mitochondria and the dynamic control of stem cell homeostasis. EMBO Rep 19:e45432.

Luo S, Valencia CA, Zhang J, Lee NC, Slone J, Gui B, Wang X, Li Z, Dell S, Brown J, Chen SM, Chien YH, Hwu WL, Fan PC, Wong LJ, Atwal PS, Huang T (2018) Biparental inheritance of mitochondrial DNA in humans. Proc Natl Acad Sci U S A doi: 10.1073/pnas.1810946115.

Margulis L (1970) Origin of eukaryotic cells. New Haven: Yale University Press.

McDonald AE, Vanlerberghe GC, Staples JF (2009) Alternative oxidase in animals: unique characteristics and taxonomic distribution. J Exp Biol 212:2627-34.

McKenzie M, Lazarou M, Thorburn DR, Ryan MT (2006) Mitochondrial respiratory chain supercomplexes are destabilized in Barth Syndrome patients. J Mol Biol 361:462-9.
Menshikova EV, Ritov VB, Fairfull L, Ferrell RE, Kelley DE, Goodpaster BH (2006) Effects of exercise on mitochondrial content and function in aging human skeletal muscle. J Gerontol A Biol Sci Med Sci 61:534-40.
Menshikova EV, Ritov VB, Ferrell RE, Azuma K, Goodpaster BH, Kelley DE (2007) Characteristics of skeletal muscle mitochondrial biogenesis induced by moderate-intensity exercise and weight loss in obesity. J Appl Physiol (1985) 103:21-7.
Menshikova EV, Ritov VB, Toledo FG, Ferrell RE, Goodpaster BH, Kelley DE (2005) Effects of weight loss and physical activity on skeletal muscle mitochondrial function in obesity. Am J Physiol Endocrinol Metab 288:E818-25.
Miller GA (1991) The science of words. Scientific American Library New York:276 pp.
Mitchell P (1961) Coupling of phosphorylation to electron and hydrogen transfer by a chemi-osmotic type of mechanism. Nature 191:144-8.
Mitchell P (2011) Chemiosmotic coupling in oxidative and photosynthetic phosphorylation. Biochim Biophys Acta Bioenergetics 1807:1507-38.
Mogensen M, Sahlin K, Fernström M, Glintborg D, Vind BF, Beck-Nielsen H, Højlund K (2007) Mitochondrial respiration is decreased in skeletal muscle of patients with type 2 diabetes. Diabetes 56:1592-9.
Mohr PJ, Phillips WD (2015) Dimensionless units in the SI. Metrologia 52:40-7.
Moreno M, Giacco A, Di Munno C, Goglia F (2017) Direct and rapid effects of 3,5-diiodo-L-thyronine (T2). Mol Cell Endocrinol 7207:30092-8.
Morrow RM, Picard M, Derbeneva O, Leipzig J, McManus MJ, Gouspillou G, Barbat-Artigas S, Dos Santos C, Hepple RT, Murdock DG, Wallace DC (2017) Mitochondrial energy deficiency leads to hyperproliferation of skeletal muscle mitochondria and enhanced insulin sensitivity. Proc Natl Acad Sci U S A 114:2705-10.
Murley A, Nunnari J (2016) The emerging network of mitochondria-organelle contacts. Mol Cell 61:648-53.
National Academies of Sciences, Engineering, and Medicine (2018) International coordination for science data infrastructure: Proceedings of a workshop—in brief. Washington, DC: The National Academies Press. doi: https://doi.org/10.17226/25015.
Oemer G, Lackner L, Muigg K, Krumschnabel G, Watschinger K, Sailer S, Lindner H, Gnaiger E, Wortmann SB, Werner ER, Zschocke J, Keller MA (2018) The molecular structural diversity of mitochondrial cardiolipins. Proc Nat Acad Sci U S A 115:4158-63.
Palmfeldt J, Bross P (2017) Proteomics of human mitochondria. Mitochondrion 33:2-14.
Paradies G, Paradies V, De Benedictis V, Ruggiero FM, Petrosillo G (2014) Functional role of cardiolipin in mitochondrial bioenergetics. Biochim Biophys Acta 1837:408-17.
Pesta D, Gnaiger E (2012) High-Resolution Respirometry. OXPHOS protocols for human cells and permeabilized fibres from small biopsies of human muscle. Methods Mol Biol 810:25-58.
Pesta D, Hoppel F, Macek C, Messner H, Faulhaber M, Kobel C, Parson W, Burtscher M, Schocke M, Gnaiger E (2011) Similar qualitative and quantitative changes of mitochondrial respiration following strength and endurance training in normoxia and hypoxia in sedentary humans. Am J Physiol Regul Integr Comp Physiol 301:R1078–87.
Price TM, Dai Q (2015) The role of a mitochondrial progesterone receptor (PR-M) in progesterone action. Semin Reprod Med 33:185-94.
Puchowicz MA, Varnes ME, Cohen BH, Friedman NR, Kerr DS, Hoppel CL (2004) Oxidative phosphorylation analysis: assessing the integrated functional activity of human skeletal muscle mitochondria – case studies. Mitochondrion 4:377-85. Puntschart A, Claassen H, Jostarndt K, Hoppeler H, Billeter R (1995) mRNAs of enzymes involved in energy metabolism and mtDNA are increased in endurance-trained athletes. Am J Physiol 269:C619-25.
Quiros PM, Mottis A, Auwerx J (2016) Mitonuclear communication in homeostasis and stress. Nat Rev Mol Cell Biol 17:213-26.
Rackham O, Mercer TR, Filipovska A (2012) The human mitochondrial transcriptome and the RNA-binding proteins that regulate its expression. WIREs RNA 3:675–95.
Rackham O, Shearwood AM, Mercer TR, Davies SM, Mattick JS, Filipovska A (2011) Long noncoding RNAs are generated from the mitochondrial genome and regulated by nuclear-encoded proteins. RNA 17:2085-93.
Reichmann H, Hoppeler H, Mathieu-Costello O, von Bergen F, Pette D (1985) Biochemical and ultrastructural changes of skeletal muscle mitochondria after chronic electrical stimulation in rabbits. Pflugers Arch 404:1-9.
Renner K, Amberger A, Konwalinka G, Gnaiger E (2003) Changes of mitochondrial respiration, mitochondrial content and cell size after induction of apoptosis in leukemia cells. Biochim Biophys Acta 1642:115-23.
Rice DW, Alverson AJ, Richardson AO, Young GJ, Sanchez-Puerta MV, Munzinger J, Barry K, Boore JL, Zhang Y, dePamphilis CW, Knox EB, Palmer JD (2016) Horizontal transfer of entire genomes via mitochondrial fusion in the angiosperm *Amborella*. Science 342:1468-73.
Rich P (2003) Chemiosmotic coupling: The cost of living. Nature 421:583.
Rich PR (2013) Chemiosmotic theory. Encyclopedia Biol Chem 1:467-72.

Roger JA, Munoz-Gomes SA, Kamikawa R (2017) The origin and diversification of mitochondria. Curr Biol 27:R1177-92.

Rostovtseva TK, Sheldon KL, Hassanzadeh E, Monge C, Saks V, Bezrukov SM, Sackett DL (2008) Tubulin binding blocks mitochondrial voltage-dependent anion channel and regulates respiration. Proc Natl Acad Sci USA 105:18746-51.

Rustin P, Parfait B, Chretien D, Bourgeron T, Djouadi F, Bastin J, Rötig A, Munnich A (1996) Fluxes of nicotinamide adenine dinucleotides through mitochondrial membranes in human cultured cells. J Biol Chem 271:14785-90.

Saks VA, Veksler VI, Kuznetsov AV, Kay L, Sikk P, Tiivel T, Tranqui L, Olivares J, Winkler K, Wiedemann F, Kunz WS (1998) Permeabilised cell and skinned fiber techniques in studies of mitochondrial function in vivo. Mol Cell Biochem 184:81-100.

Salabei JK, Gibb AA, Hill BG (2014) Comprehensive measurement of respiratory activity in permeabilized cells using extracellular flux analysis. Nat Protoc 9:421-38.

Sazanov LA (2015) A giant molecular proton pump: structure and mechanism of respiratory complex I. Nat Rev Mol Cell Biol 16:375-88.

Schneider TD (2006) Claude Shannon: biologist. The founder of information theory used biology to formulate the channel capacity. IEEE Eng Med Biol Mag 25:30-3.

Schönfeld P, Dymkowska D, Wojtczak L (2009) Acyl-CoA-induced generation of reactive oxygen species in mitochondrial preparations is due to the presence of peroxisomes. Free Radic Biol Med 47:503-9.

Schultz J, Wiesner RJ (2000) Proliferation of mitochondria in chronically stimulated rabbit skeletal muscle--transcription of mitochondrial genes and copy number of mitochondrial DNA. J Bioenerg Biomembr 32:627-34.

Simson P, Jepihhina N, Laasmaa M, Peterson P, Birkedal R, Vendelin M (2016) Restricted ADP movement in cardiomyocytes: Cytosolic diffusion obstacles are complemented with a small number of open mitochondrial voltage-dependent anion channels. J Mol Cell Cardiol 97:197-203.

Singh BK, Sinha RA, Tripathi M, Mendoza A, Ohba K, Sy JAC, Xie SY, Zhou J, Ho JP, Chang CY, Wu Y, Giguère V, Bay BH, Vanacker JM, Ghosh S, Gauthier K, Hollenberg AN, McDonnell DP, Yen PM (2018) Thyroid hormone receptor and ERRα coordinately regulate mitochondrial fission, mitophagy, biogenesis, and function. Sci Signal 11(536) DOI: 10.1126/scisignal.aam5855.

Speijer D (2016) Being right on Q: shaping eukaryotic evolution. Biochem J 473:4103-27.

Stucki JW, Ineichen EA (1974) Energy dissipation by calcium recycling and the efficiency of calcium transport in rat-liver mitochondria. Eur J Biochem 48:365-75.

Sugiura A, Mattie S, Prudent J, McBride HM (2017) Newly born peroxisomes are a hybrid of mitochondrial and ER-derived pre-peroxisomes. Nature 542:251-4.

Tonkonogi M, Harris B, Sahlin K (1997) Increased activity of citrate synthase in human skeletal muscle after a single bout of prolonged exercise. Acta Physiol Scand 161:435-6.

Torralba D, Baixauli F, Sánchez-Madrid F (2016) Mitochondria know no boundaries: mechanisms and functions of intercellular mitochondrial transfer. Front Cell Dev Biol 4:107. eCollection 2016.

Vamecq J, Schepers L, Parmentier G, Mannaerts GP (1987) Inhibition of peroxisomal fatty acyl-CoA oxidase by antimycin A. Biochem J 248:603-7.

Waczulikova I, Habodaszova D, Cagalinec M, Ferko M, Ulicna O, Mateasik A, Sikurova L, Ziegelhöffer A (2007) Mitochondrial membrane fluidity, potential, and calcium transients in the myocardium from acute diabetic rats. Can J Physiol Pharmacol 85:372-81.

Wagner BA, Venkataraman S, Buettner GR (2011) The rate of oxygen utilization by cells. Free Radic Biol Med 51:700-712.

Wang H, Hiatt WR, Barstow TJ, Brass EP (1999) Relationships between muscle mitochondrial DNA content, mitochondrial enzyme activity and oxidative capacity in man: alterations with disease. Eur J Appl Physiol Occup Physiol 80:22-7.

Watt IN, Montgomery MG, Runswick MJ, Leslie AG, Walker JE (2010) Bioenergetic cost of making an adenosine triphosphate molecule in animal mitochondria. Proc Natl Acad Sci U S A 107:16823-7.

Weibel ER, Hoppeler H (2005) Exercise-induced maximal metabolic rate scales with muscle aerobic capacity. J Exp Biol 208:1635–44.

White DJ, Wolff JN, Pierson M, Gemmell NJ (2008) Revealing the hidden complexities of mtDNA inheritance. Mol Ecol 17:4925–42.

Wikström M, Hummer G (2012) Stoichiometry of proton translocation by respiratory complex I and its mechanistic implications. Proc Natl Acad Sci U S A 109:4431-6.

Williams EG, Wu Y, Jha P, Dubuis S, Blattmann P, Argmann CA, Houten SM, Amariuta T, Wolski W, Zamboni N, Aebersold R, Auwerx J (2016) Systems proteomics of liver mitochondria function. Science 352 (6291):aad0189

Willis WT, Jackman MR, Messer JI, Kuzmiak-Glancy S, Glancy B (2016) A simple hydraulic analog model of oxidative phosphorylation. Med Sci Sports Exerc 48:990-1000.

Yoshinaga MY, Kellermann MY, Valentine DL, Valentine RC (2016) Phospholipids and glycolipids mediate proton containment and circulation along the surface of energy-transducing membranes. Prog Lipid Res 64:1-15.

Zíková A, Hampl V, Paris Z, Týč J, Lukeš J (2016) Aerobic mitochondria of parasitic protists: diverse genomes and complex functions. Mol Biochem Parasitol 209:46-57.

Supplement

S1. Manuscript phases and versions - an open-access apporach

This manuscript on 'Mitochondrial respiratory states and rates' is a position statement in the frame of COST Action CA15203 MitoEAGLE. The global MitoEAGLE network made it possible to collaborate with a large number of coauthors to reach consensus on the present manuscript. Nevertheless, we do not consider scientific progress to be supported by 'declaration' statements (other than on ethical or political issues). Our manuscript aims at providing arguments for further debate rather than pushing opinions. We hope to initiate a much broader process of discussion and want to raise the awareness of the importance of a consistent terminology for reporting of scientific data in the field of bioenergetics, mitochondrial physiology and pathology. Quality of research requires quality of communication. Some established researchers in the field may not want to re-consider the use of jargon which has become established despite deficiencies of accuracy and meaning. In the long run, superior standards will become accepted. We hope to contribute to this evolutionary process, with an emphasis on harmonization rather than standardization.

Phase 1 The protonmotive force and respiratory control
http://www.mitoeagle.org/index.php/The_protonmotive_force_and_respiratory_control

- 2017-04-09 to 2017-09-18 (44 versions) / 2017-09-21 to 2018-02-06 (44 plus 21 versions)
  http://www.mitoeagle.org/index.php/MitoEAGLE_preprint_2017-09-21
  2017-11-11: Print version (16) for MiP2017/MitoEAGLE conference in Hradec Kralove

Phase 2 Mitochondrial respiratory states and rates: Building blocks of mitochondrial physiology Part 1
http://www.mitoeagle.org/index.php/MitoEAGLE_preprint_States_and_rates

- 2018-02-08 – 2019-01-24 (44 plus 52 traceable Versions)

Phase 3 2019-02-12 Preprint DOI number doi:10.26124/mitofit:190001
2019-03-15 Version 2: doi:10.26124/mitofit:190001.v2
2019-04-24 Version 3: doi:10.26124/mitofit:190001.v3
2019-05-20 Version 4: doi:10.26124/mitofit:190001.v4

Phase 4 Journal submission

S2. Joining COST Actions

- CA15203 MitoEAGLE - http://www.cost.eu/COST_Actions/ca/CA15203
- CA16225 EU-CARDIOPROTECTION - http://www.cost.eu/COST_Actions/ca/CA16225
- CA17129 CardioRNA - http://www.cost.eu/COST_Actions/ca/CA17129

S3. COST Action CA15203 MitoEAGLE

COST Action
CA15203
MitoEAGLE
Evolution **A**ge **G**ender
Lifestyle **E**nvironment

Mission of the global MitoEAGLE network

in collaboration with the Mitochondrial Physiology Society, MiP*s*

- Improve our knowledge on mitochondrial function in health and disease with regard to **E**volution, **A**ge, **G**ender, **L**ifestyle and **E**nvironment
- Interrelate studies across laboratories with the help of a MitoEAGLE data management system
- Provide standardized measures to link mitochondrial and physiological performance to understand the myriad of factors that play a role in mitochondrial physiology

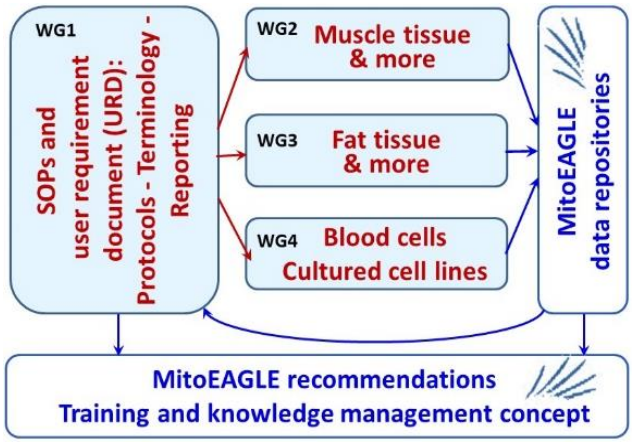

Join the COST Action MitoEAGLE - contribute to the quality management network.

More information:
www.mitoeagle.org

EUROPEAN COOPERATION IN SCIENCE & TECHNOLOGY

Funded by the Horizon 2020 Framework Programme of the European Union